The Canadian Mineralogist
Vol. 42, pp. 1777-1798 (2004)

THE ORIGIN OF BULK AND WATER-SOLUBLE Cl AND Br ENRICHMENTS IN ORE-HOSTING SUDBURY BRECCIA IN THE FRASER COPPER ZONE, STRATHCONA EMBAYMENT, SUDBURY, ONTARIO, CANADA

Jacob J. HANLEY[§], James E. MUNGALL, Colin J. BRAY and Michael P. GORTON

Department of Geology, University of Toronto, 22 Russell Street, Toronto, Ontario M5S 3B1, Canada

Abstract

The transition from barren Sudbury Breccia to Sudbury Breccia zones hosting footwall Cu–Ni–PGE sulfide ore at the Fraser mine, Ontario, is accompanied by an increase in the concentration of bulk-rock Cl and Br and water-soluble (at 20°C) Cl and Br and in the Cl:Br ratio in the matrix (pseudotachylite) of the breccia. Anomalous bulk-rock concentrations of Cl (1.5–10 times background) and Br (1.5–2 times background) are detectable for distances of at least 150 m away from the first visible signs of footwall sulfide mineralization. The Cl:Br ratio in the bulk rock increases with proximity to ore, reflecting the increasing abundance of Cl-bearing and Br-excluding silicate minerals in the matrix of the breccias. Up to ~70% of the Cl (on average, 35–40%) and ~80% of the Br (on average, 25–35%) in Sudbury Breccia matrix are water-soluble at room temperature, and reside in (i) primary fluid inclusions along recrystallized grain-boundaries, which increase in abundance with proximity to ore, and (ii) halite crystals in pore spaces and vugs in the matrix. Aqueous solutions prepared by leaching powdered samples of the matrix of the Sudbury Breccia exhibit variable Ca:Na and Cl:Br ratios, which may be explained partly by the precipitation of small amounts of halite ($<10^{-5}$ wt% of the bulk rock) in pore spaces and vugs within the matrix of the breccia by parental groundwaters. As an alternative, the range in leachate compositions may be explained by the presence of trapped mixtures (in fluid inclusions) of Ca-dominant groundwater and a Na- and K-dominant fluid that had elevated and variable Cl:Br ratios, possibly exsolved from the SIC (Sudbury Igneous Complex). In general, elevated bulk Cl and Br, water-soluble Cl and Br, and bulk Cl:Br ratio are reliable indicators of proximity to footwall Cu–Ni–PGE sulfide mineralization, particularly in samples devoid of disseminated sulfide or where sulfide minerals are sparse.

Keywords: halogens, cations, chlorine, bromine, Sudbury Breccia, hydrothermal, alteration, fluid inclusions, groundwater, Sudbury Igneous Complex, Ontario.

Sommaire

La transition entre les domaines où la brèche de Sudbury est stérile et ceux où elle renferme un minerai à sulfures de Cu–Ni–PGE à la mine Fraser, en Ontario, est accompagnée d'une augmentation de la concentration de Cl et de Br dans les roches globales, dans la fraction possible à dissoudre dans l'eau (à 20°C), et du rapport Cl:Br dans la matrice (pseudotachylite) de la brèche. Nous pouvons détecter des concentrations anomales de Cl et de Br dans les roches totales (1.5–10 et 1.5–2 fois le bruit de fond, respectivement) sur des distances d'au moins 150 m des premiers indices visibles de minéralisation en sulfures dans les roches du socle. Le rapport Cl:Br dans la roche globale augmente en s'approchant des zones minéralisées, témoignant de l'augmentation dans la proportion des minéraux aptes à accepter le Cl et à exclure le Br. Jusqu'à ~70% du Cl (en moyenne, 35–40%) et ~80% du Br (en moyenne, 25–35%) dans la matrice de la brèche de Sudbury sont solubles dans l'eau à température ambiante, et résident (i) dans des inclusions fluides primaires le long des interfaces recristallisées entre grains, qui augmentent en s'approchant du minerai, et (ii) dans des cristaux de halite dans les vacuoles et les pores de la matrice. Des solutions aqueuses préparées par lessivage des échantillons de la matrice de la brèche pulvérisés indiquent les rapports Ca:Na et Cl:Br variables, qui seraient en partie le résultat de précipitation d'infimes quantités de halite ($<10^{-5}$% du poids de la roche totale) dans les pores et les vacuoles de la matrice par des eaux souterraines. Comme alternative, on peut aussi expliquer la composition de la fraction lessivée en proposant la présence de mélanges piégés (dans les inclusions fluides) d'eau souterraine, à dominance de Ca, et d'un fluide à dominance de Na et K ayant un rapport Cl:Br élevé mais variable, qui serait issu du complexe igné de Sudbury. En général, les teneurs élevées de Cl et Br des roches globales, de la fraction soluble, et le rapport Cl:Br élevé des échantillons de matrice seraient des indicateurs fiables de la proximité à la minéralisation en sulfures de Cu–Ni–PGE, particulièrement dans le cas d'échantillons dépourvus de sulfures disséminés ou bien où ceux-ci sont épars.

(Traduit par la Rédaction)

Mots-clés: halogènes, cations, chlore, brome, brèche de Sudbury, hydrothermal, altération, inclusions fluides, eau souterraine, complexe igné de Sudbury, Ontario.

[§] *E-mail address*: hanley@geology.utoronto.ca

INTRODUCTION

The highly mobile and volatile nature of chlorine and bromine in most geological environments (*e.g.*, geothermal systems, igneous-rock-forming systems, sedimentary basins) makes an accurate determination of the distribution and concentration of these elements in parent magmas or fluids difficult. As a result, the use of the Cl:Br ratio in modeling groundwater and fluid evolution has been widely established because of the highly conservative nature of Cl and Br in low-temperature aqueous geochemical systems, and the constancy of the Cl:Br ratio in fluids unless altered by specific, well-characterized processes (*e.g.*, halide precipitation, mixing and dilution of basinal brines). At higher temperatures, in hydrothermal and magmatic regimes, the Cl:Br ratio in a fluid may be altered owing to phase changes (*e.g.*, boiling, vapor condensation) or the growth of minerals that incorporate Cl and exclude Br (*e.g.*, apatite, biotite, hornblende, sodalite).

In this study, we examine the distribution of bulk-rock and water-soluble Cl and Br in the aphanitic matrix of a rock type known as the Sudbury Breccia, which occurs at the Fraser mine along the northern margin of the Sudbury Igneous Complex (SIC), in central Ontario. This rock type is a major host to the footwall-type sulfide mineralization involving Cu, Ni, and the platinum-group elements (PGE) in the Sudbury mining camp. With the aid of Cl:Br ratios, we discuss the distribution of bulk Cl, Br, and soluble Cl^-, Br^- and associated cations in the matrix of the Sudbury Breccia in relation to possible sources of fluid, and demonstrate that the bulk and water-soluble (at room temperature) Cl^- and Br^- content of Sudbury Breccia matrix may be used to discriminate between barren and mineralized zones of Sudbury Breccia on the northern margin of the Sudbury Igneous Complex (SIC).

BACKGROUND

Geological setting of the study

The Fraser mine (Falconbridge Ltd.) is located along the northern edge of the Sudbury Igneous Complex (SIC), approximately 60 km north of the city of Sudbury, in Levack Township, Ontario (Fig. 1). The SIC is a Proterozoic igneous body considered to be the product of a meteorite impact at 1849 Ma BP (Dietz 1964, Krogh *et al.* 1984, Grieve 1994). At the Fraser mine, the SIC forms a tabular sheet dipping to the southeast, composed of noritic to dioritic cumulates overlain by a granophyric residuum. Along the basal contact of the SIC, partially melted target rocks comprise an igneous-textured footwall breccia (locally called "late granite breccia"). At the Fraser mine, the footwall breccia overlies Archean gneisses, granites, migmatites, and diabase dykes of the Superior Province. During impact, the excavation, brecciation, and melting of the footwall rocks at the Fraser mine created structural traps along the basal contact of the SIC in which contact-style Ni–Cu–PGE sulfide deposits were introduced during the differentiation of the SIC. Magmatic differentiation of the sulfide liquid along the lower contact of the SIC resulted in the formation of residual sulfide liquid enriched in Cu, Pt, Pd and Au. This Cu-rich sulfide liquid then settled into zones of brecciated gneissic rock (Sudbury Breccia) in the footwall to the SIC to form footwall-style Cu–Ni–PGE sulfide deposits (*e.g.*, Li 1992, Li & Naldrett 1993, Morrison *et al.* 1994).

Characteristics of the Sudbury Breccia

The Sudbury Breccia is one of several types of "breccia" associated with the Sudbury impact structure. It was produced during impact-induced seismogenic faulting (Spray 1997). The matrix of the Sudbury Breccia is composed of pseudotachylite (Dressler 1984), which closely resembles the type-locality pseudotachylite at the Vredefort impact structure in South Africa (Shand 1916, Wilshire 1971). The pseudotachylite matrix is preserved as very fine-grained, diabasic-textured to equigranular material, reflecting its probable origin by frictional melting of wallrocks. The matrix encloses locally derived angular to rounded clasts. Near the SIC and in proximity to footwall mineralization, the Sudbury Breccia has been recrystallized and altered by contact metamorphism and hydrothermal processes (Coats & Snajdr 1984, Dressler 1984, Farrow 1994, Morrison *et al.* 1994, Hanley & Mungall 2003). The greatest volumes of Sudbury Breccia are found surrounding and along the surfaces of the structurally complex depressions of the footwall contact beneath the SIC, which host the footwall-style sulfide mineralization described above (Cowan 1968, Morrison *et al.* 1994, Fedorowich *et al.* 1999). The zones of Sudbury Breccia that host footwall-style Cu–Ni–PGE mineralization at the Fraser mine occur below the Strathcona embayment, subparallel to the embayment axis, which plunges approximately 21° SSW (Fedorowich *et al.* 1999) (Fig. 2a). The occurrence of footwall Cu–Ni–PGE sulfide mineralization within zones of Sudbury Breccia indicates that the breccia bodies served as conduits or structural traps for migrating batches of sulfide liquid or metal-bearing hydrothermal fluid (Morrison *et al.* 1994, Farrow 1994).

REVIEW OF PREVIOUS WORK

Several investigators have characterized the distribution of halogens in fluid inclusions and assemblages of alteration minerals associated with footwall Cu–Ni–PGE and contact Ni–Cu–PGE ores at Sudbury (Buchan 1981, Springer 1989, Farrow & Watkinson 1992, 1996, 1997, 1999, Li 1992, Li & Naldrett 1993, Jago *et al.* 1994, Farrow 1994, Marshall *et al.* 1999, McCormick & McDonald 1999, Molnár *et al.* 2001, McCormick *et al.* 2002, Hanley 2002, Hanley & Mungall 2003). These investigators have demonstrated that multiple hydrothermal events occurred in the footwall of the SIC during its crystallization and cooling, and were partially responsible for the primary deposition and secondary remobilization of base and precious metals. Primary, high-salinity aqueous fluid associated with the earliest hydrothermal event may be (i) exsolved magmatic fluid (*i.e.*, expelled from the crystallizing SIC melt sheet or a sulfide melt: Li 1992, Molnár *et al.* 2001), (ii) hypersaline Ca–Na–Cl-rich groundwater of the Canadian Shield (Frape & Fritz 1982, 1987, Pearson 1985), which was modified by fluid – host-rock interaction prior to or during ore formation (Farrow 1994), or (iii) a mixture of SIC-exsolved magmatic fluid and groundwater (Marshall *et al.* 1999).

A few investigators have observed elevated bulk-rock concentrations of Cl and high Cl:F and K:Na ratios in the host rocks to footwall-style Cu–Ni–PGE ores and contact-style Ni–Cu–PGE ores at the McCreedy East and Fraser mines (Jago *et al.* 1994, McCormick *et al.* 2002). Also, Hanley & Mungall (2003) showed that bulk enrichment in Cl in the Sudbury Breccia hosting footwall Cu–Ni–PGE deposits is associated with elevated modal abundances of Cl-bearing hydroxysilicate minerals (biotite, actinolite, and chlorite) and enrichment in the Cl content of these minerals in proximity to footwall-style mineralization. The origin of these alteration haloes was attributed to the interaction of late-stage magmatic fluids and the host rocks to ore near the contact of the SIC (McCormick *et al.* 2002) and to retrograde metamorphic processes unique to Sudbury Breccia zones that host footwall-style ores (Hanley & Mungall 2003).

SAMPLING AND SAMPLE PREPARATION

Samples of Sudbury Breccia matrix were obtained from three underground settings (Figs. 1, 2a–b): (i) drift walls in stope #1620 of Zone 38 of the Fraser Copper Zone, 3700 foot level (1130 m), Fraser mine, (ii) haulage drifts and ramps in the footwall and hanging wall of Zone 38, 3700 foot level (1130 m), Fraser mine, and (iii) surface drill-hole NRD60 (near the Fraser mine) and underground drill-hole OD49081 (from the Craig mine), which intersected zones of barren (unmineralized) Sudbury Breccia at depths of 1430–1460 m, and 900–1025 m, respectively. Samples from surface exposures were not used in this study since surficial weathering removes Cl in preference to Br at depths of up to 1 m in apparently fresh rock, thereby masking any true geochemical signatures related to proximity to mineralization (Hanley 2002). The samples were classified according to their proximity to the first visible signs of footwall Cu–Ni–PGE sulfide mineralization, and occurrence either within or outside a Sudbury Breccia zone known to host footwall sulfide ore. Three sample divisions (distal, peripheral, and proximal) were used: *distal* Sudbury Breccia matrix was sampled from the drill holes intersecting unmineralized zones of Sudbury Breccia at distances of greater than 150 m from known mineralization; *peripheral* breccia matrix was sampled within an ore-hosting breccia zone at distances of 10 to 150 m from mineralization (haulage drifts and ramps); *proximal* breccia matrix was sampled within an ore-hosting breccia zone at distances of less than 10 m from mineralization (active mine headings). The mineralogical characteristics of matrix samples classified as *distal* should be considered as being representative of background conditions unrelated to mineralization. A detailed explanation of the sample-classification method can be found in Hanley & Mungall (2003).

Ninety-seven samples of Sudbury Breccia were collected from the three study areas described. At each sample site or drill-core interval, several chips (totaling ~1 kg mass) were collected over a large area (~1 m^2) or core length (~0.5 m) to help minimize sample-scale heterogeneity. Samples of Sudbury Breccia were collected containing clasts and fragments of country rock less than ~0.5 cm in size. Clasts larger than ~0.5 cm contain sufficient volume of fresh, unaltered country-rock at their cores to introduce significant chemical heterogeneity in trace-element populations (Hanley 2002), and were cut out by diamond saw prior to pulverization. Samples were crushed in a chromium steel jaw crusher, rinsed in hot (80°C) 1M nitric acid (Optima™ grade) followed by a rinse with deionized water to remove any halogen-bearing surface contaminants, and pulverized for 2 minutes using an alumina-lined puck mill (70% grains sized <50 μm).

ANALYTICAL METHODS

Small chips of Sudbury Breccia matrix from each group of samples were mounted, broken open, and the opened surfaces examined by scanning electron microscope (JEOL, JSM–840) in order to identify and characterize sites of deposition of halogen-bearing condensates in fluid inclusions, pore spaces, and vugs. Observations were made of recrystallized mineral grains in the matrix, and of clasts of gneissic host-rock, which form a physical continuum with the matrix at increasingly smaller clast sizes. Thin sections were also used to characterize the types of inclusions.

Bulk Cl and Br were quantified by wavelength-dispersion (WD) X-ray fluorescence spectrometry (XRF, Philips 2404) on 28-mm-diameter pressed-powder pellets (Department of Geology, University of Toronto). The calibration lines for the halogens were obtained using dilutions (in a granitic matrix) of the international reference standard MAG–1 (U.S.G.S. marine mud), synthetic standards composed of salt solutions (KCl and KBr) of known concentration diluted in silica powder, and salt reagents (KCl and NaCl) containing natural and artificial Br impurities determined previously by ion

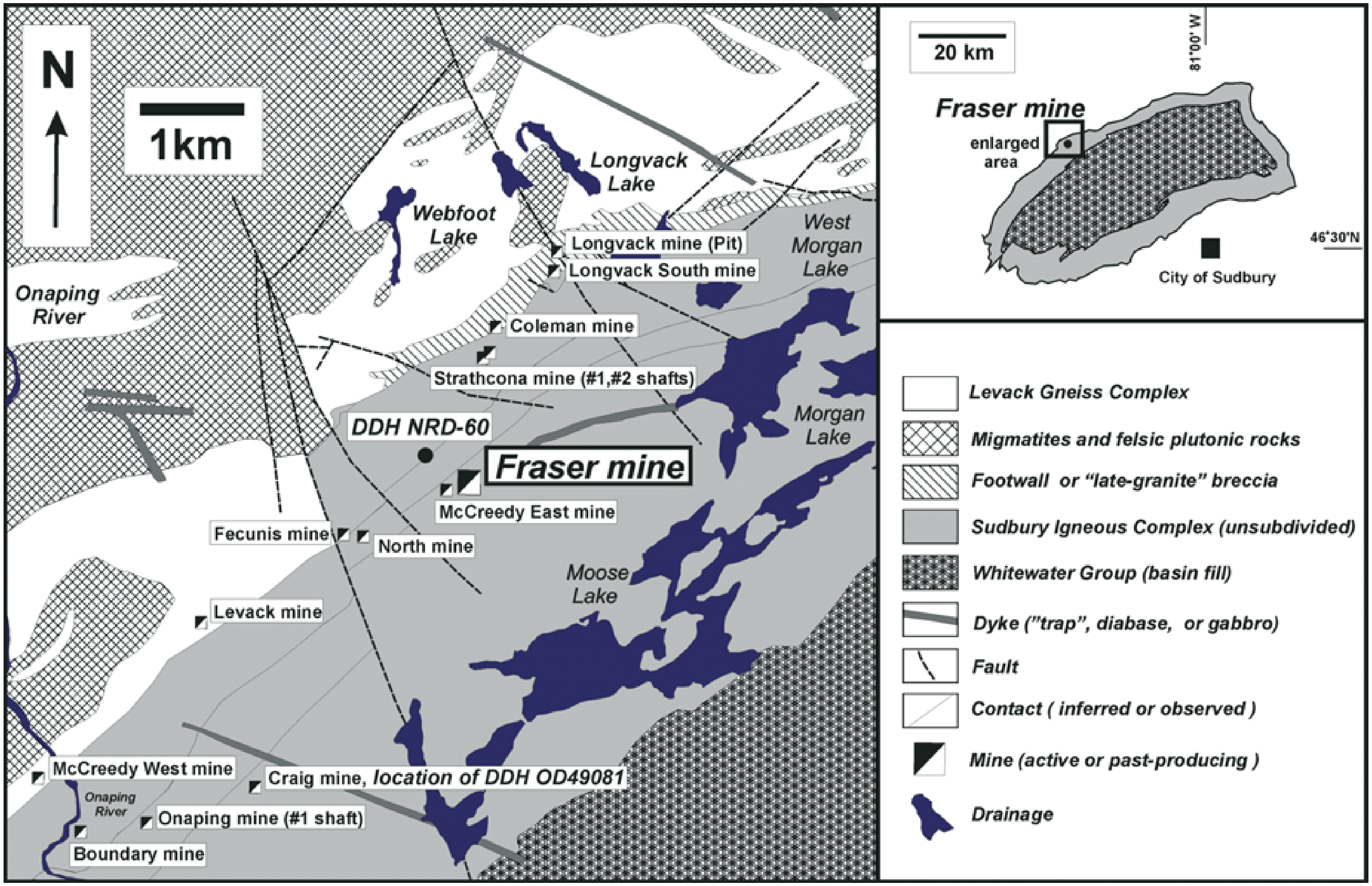

FIG. 1. Generalized geology of the area surrounding the Fraser mine on the northwestern margin of the Sudbury Igneous Complex (SIC), showing the location of past and currently producing mines, and locations of drill holes from which the core samples analyzed in this study were taken. Inset image shows the location of the Fraser mine relative to the entire Sudbury Igneous Complex and the city of Sudbury.

chromatography (Department of Geology, University of Toronto). Routine limits of detection (3σ) for Cl and Br were 5 ppm and 0.65 ppm, respectively.

Aqueous leachates (containing Ca^{2+}, Mg^{2+}, Na^+, K^+, Cl^-, Br^-, SO_4^{2-}) were analyzed in the F. Gordon Smith Fluid Inclusion Laboratory at the University of Toronto by ion chromatography (Channer *et al.* 1994). Leachates were prepared from 36 pulverized Sudbury Breccia matrix samples. The method used to prepare the leachates is comparable to that used for fluid-inclusion leachates from quartz and is reported in Channer *et al.* (1994). Leachate solutions were analyzed using a semi-automated DIONEX 2000i – SP ion chromatograph with post-column conductivity suppression and an electrical conductivity detector linked to a PC with chromatograph collection and analysis software. Anions (Cl^-, Br^-, SO_4^{2-}) were separated on DIONEX AG9 guard and AS9 separation columns carried by an eluent mixture of 2 mM Na_2CO_3 + 0.75 mM $NaHCO_3$ at a flow rate of 1.8 mL/min. Cations (Na^+, K^+, Mg^{2+}, Ca^{2+}) were separated on DIONEX CG12 guard and CS12 separation columns carried in an eluent of 20 mM H_2SO_4 at a flow rate of 1.0 mL/min. Calibration was performed using in-house alkali halide standard solutions. It was determined by repeated leaching experiments that the two minutes of pulverization succeeded in liberating (for

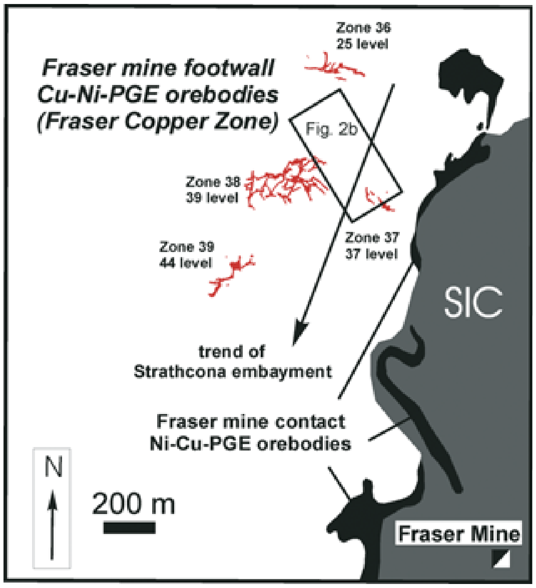

FIG. 2. a. Plan view of the Fraser mine orebodies projected to the 762 (meter) level. Note that the SIC has been greatly simplified to included the footwall or "late granite" breccia, which hosts some of the contact-style Ni–Cu–PGE ore (shown in black along the SIC contact). Representative cross-cuts for the four footwall-style Cu–Ni–PGE ore zones (36–38) are shown in red; these zones lie beneath the Strathcona embayment, which trends to the south-southwest, plunging approximately 21°. The study area (box; enlarged in Fig. 2b) includes the hanging wall of Zone 37 and the northeastern portion of Zone 38.

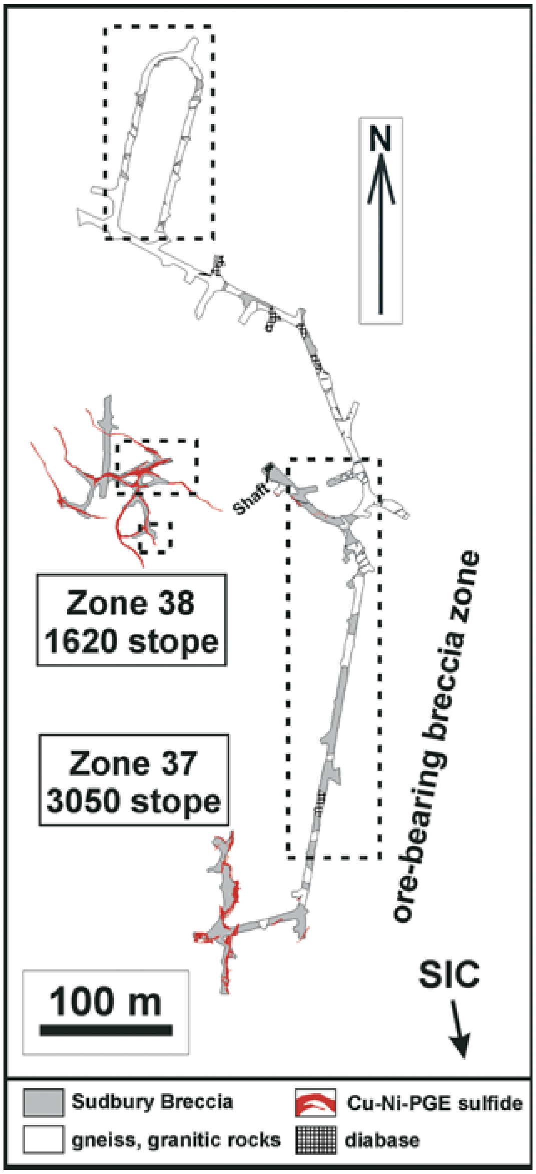

FIG. 2. b. Drift walls in the Fraser Copper Zone study area projected to the 3700 foot level, showing mine geology (simplified) around Zones 37 and 38. The ore-hosting breccia zone is comprised of 46% brecciated gneissic rocks. Breccia abundance decreases to less than 18% in the footwall of Zone 38 (northeast of Zone 38). Dashed boxes are areas where drift walls were sampled (at 5–10 m spacings between samples).

leaching purposes) at least 95% of the soluble Cl and Br present in the bulk sample. A more detailed description of the analytical procedure and instrumentation can be found in Channer *et al.* (1994) and Hanley (2002).

RESULTS: HALOGEN-BEARING FLUID INCLUSIONS AND SALT CRYSTALS IN THE MATRIX OF THE SUDBURY BRECCIA

Secondary, $L_{aq} + V \pm nS \pm L_{carbonic}$ (*type-Ia, -Ib, and -Ic*)

Secondary inclusions were observed in quartz and plagioclase within the "fresh", unrecrystallized cores of gneissic clasts and in quartz patches in samples from all three divisions (Figs. 3a, b). The abundance of these secondary inclusions is very low relative to populations of type-II inclusions in the breccia matrix (see below) and does not vary with proximity to ore. They were classified as secondary in origin because of their occurrence within single mineral grains as trails associated with healed or partly healed fracture planes (Roedder 1984). The inclusions range from 0.5 to 10 μm in size (average size 1–2 μm). Three different types of secondary inclusions were observed, each defining a genetically distinct population. In type-Ia inclusions, an aqueous liquid and small vapor bubble (<15 vol.%) are invariably present. In type-Ib inclusions, an aqueous liquid and a larger vapor bubble are present, and up to 80% of the inclusions of this type contain solid phases. Solid phases (Figs. 4a–c), identified by SEM–EDS in opened inclusions and on fracture surfaces immediately adjacent to the inclusions, are chlorides of Na and Ca, and rarely K. Halite was the most common solid phase observed. A variety of accidentally trapped solid phases were identified in type-Ib inclusions, the most common being calcite, feldspars, micas, and chalcopyrite. Type-Ic inclusions contain aqueous liquid, carbonic liquid, and vapor. Although no microthermometry was performed in this study, the occurrence of three types of secondary inclusions is consistent with detailed fluid-inclusion petrography and microthermometry performed by Molnár *et al.* (2001) on samples from the SIC footwall. They reported secondary $L_{aq} + L_{carbonic} + V$, $L_{aq} + V + S_{halite}$, and $L_{aq} + V$ ($V < 20$ vol.%) inclusions occurring in late calcite – quartz – epidote – actinolite veinlets and rock-forming quartz in the Levack Gneiss.

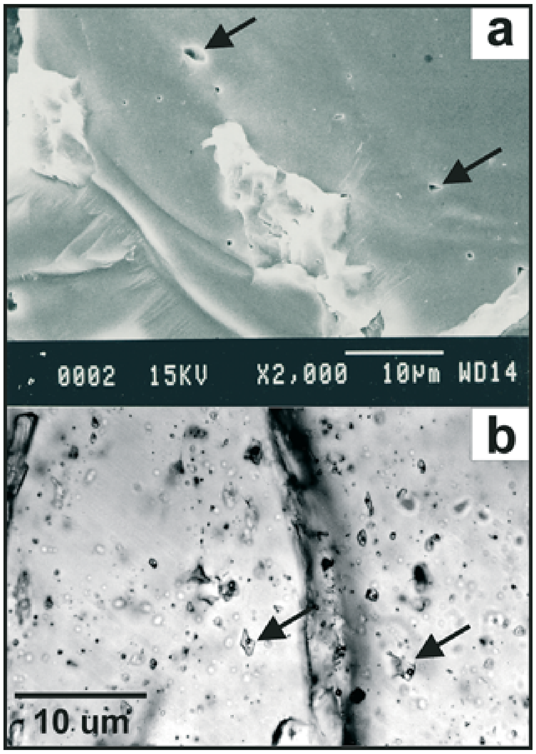

FIG. 3. Secondary fluid inclusions in Sudbury Breccia. a. Secondary electron image of a coated fracture-surface showing trails of opened secondary inclusions in a gneissic clast. b. Image in transmitted, plane-polarized light image showing type-Ib secondary inclusions containing an aqueous liquid, vapor bubble, and halite cube.

Primary , $L + V \pm n\,S$ (*type II*)

Abundant fluid inclusions were observed along healed or partially healed grain-boundaries (*not* fracture planes) in patches of quartz within Sudbury Breccia matrix (Figs. 5a–b). The patches of quartz have been described previously as the product of extensive recrystallization, anatexis, and retrograde metamorphism of the Sudbury Breccia during formation, subsequent metamorphism by the SIC, and alteration associated with footwall ore-forming processes (Morrison *et al.* 1994, Hanley 2002, Hanley & Mungall 2003). Healed interfaces between grains that contain type-II inclusions are commonly cross-cut by fractures containing type-I inclusions. Type-II inclusions were classified as primary in origin with respect to their host quartz because they fit the criteria for primary intercrystalline inclusions that are not hosted in a single crystal but form along communal growth-surfaces between two separate, adjacent grains (Roedder 1984). Type-II inclusions are small (<4 μm, average 2 μm), and contain an aqueous liquid, a large vapor bubble, and commonly a solid phase. Vapor-to-liquid ratios are somewhat variable, ranging from 50 to 80 vol.%. The inclusions are commonly poorly formed and exhibit incomplete healing (inclusions are empty). For example, those inclusions occurring along exposed grain-boundary surfaces were observed to be commonly interconnected to adjacent inclusions by smooth, crescent-shaped, or bifurcating tubes or channels (Fig. 5b). Type-II inclusions were not observed in trails (healed fracture-planes). Solid phases were observed in approximately 40% of type-II inclusions as subhedral to euhedral crystals of Na, Ca, and K chlorides (identified by SEM–EDS), which fill between 20 and 70% of the inclusion volume. Inclusion walls typically envelop the salt crystals very tightly or the salt crystals occur partially embedded in the inclusion walls. This textural observation, combined with the rarity of solid salt phases and highly variable fill-ratios where they occur, suggest that these solid phases are accidental phases trapped along the grain boundaries during recrystallization of the quartz. Quartz precipitation onto inclusion walls probably continued after the solid phases were trapped, but before the inclusions were sealed. Where solid phases are absent, analyses of the "quenched" precipitate around the margins of opened inclusions by SEM–EDS indicate the presence of Na, Ca, and K in the inclusion fluids.

Type-II inclusions show a definite increase in abundance with increasing proximity to mineralization. Estimates of the relative abundance of type-II inclusions from thin sections were made using digital photomicrographs and image analysis software (Scion Image®). The results of that exercise showed that type-II inclusions account for approximately 90% (by volume) of the trapped fluid in fluid inclusions in the breccia samples, and peripheral and proximal samples contain two to five times the number of type-II inclusions compared to distal samples. Type-I inclusions account for the remaining ~10% (by volume). Type-II inclusions are considered to have formed during grain-boundary migration corresponding to the recrystallization and annealing of mineral grains in the breccia matrix. In addition to hosting the type-II inclusions, former grain-boundaries in quartz show complex but equilibrium (mutual) intergrowths with Cl-bearing alteration minerals such as actinolite and biotite. Texturally, the recrystallization of quartz and feldspars within the matrix that hosts type-II inclusions appears to have coincided with the growth of abundant Cl-bearing hydroxysilicate phases (Hanley & Mungall 2003). Such processes have

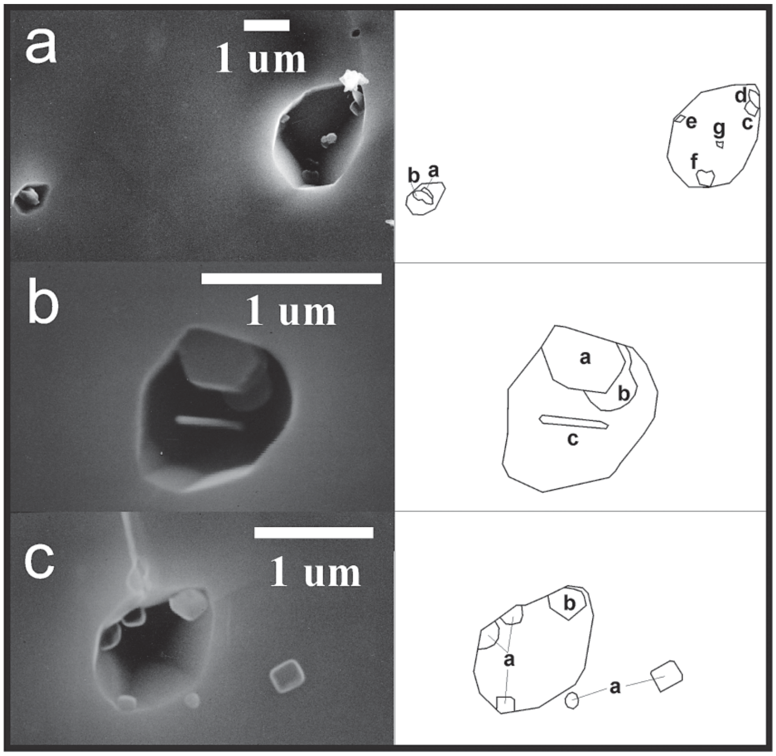

FIG. 4. Secondary electron images of opened type-Ib secondary inclusions containing solid phases characterized by SEM–EDS. a. Labeled solid phases contain (a) K–Al–Si (K-feldspar), (b) Ca–Cl, (c) Na–(K)–Cl, (d) and (e) Ca–(Na)–(K)–Cl, (f) K–Fe–Mg–Al–Si (biotite or amphibole?), and (g) Na–Cl. b. (a) Ca–(Na)–Cl, (b) Na–Cl, and (c) K–Fe–Mg–Al–Si (biotite or amphibole?). c. (a) Na–(K)–Cl and (b) Ca–Cl.

been shown to be more intensely developed in breccia zones that now host footwall-style deposits (Jago *et al.* 1994, Morrison *et al.* 1994, Hanley 2002, Hanley & Mungall 2003). Thus, the origin of type-II inclusions is considered primary with respect to the retrograde metamorphism of Sudbury Breccia matrix associated with emplacement of footwall mineralization (Hanley & Mungall 2003). Inclusions exhibiting this textural association were previously unreported by Molnár *et al.* (2001). In the absence of microthermometry, the rarity of solid phases in type-II inclusions, consistently large volume of vapor phase, and unique textural setting are interpreted as indicators that type-II inclusions are not the equivalent of any of the type-I inclusions reported here, nor the primary, high-salinity polyphase inclusions of magmatic origin reported by Molnár *et al.* (2001). Furthermore, healed grain-boundaries now occupied by type-II inclusions are commonly cross-cut by type-I inclusions, an indication that type-II inclusions are older.

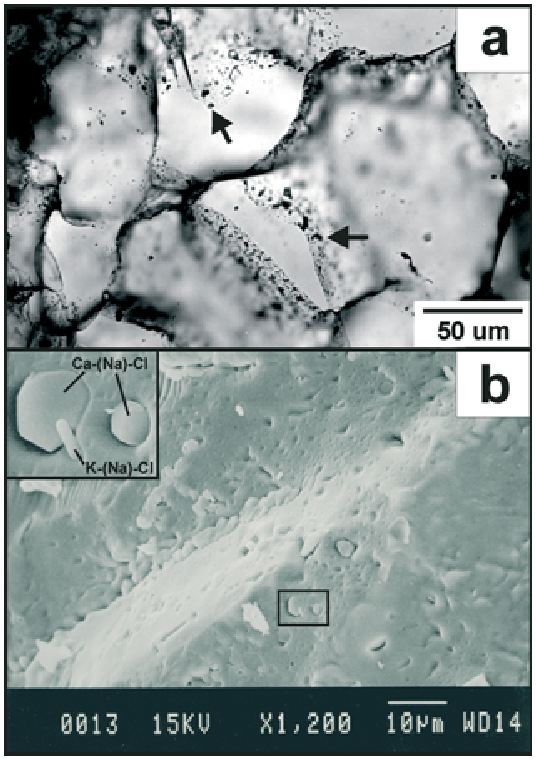

FIG. 5. Primary fluid inclusions in Sudbury Breccia. a. Image in transmitted, plane-polarized light of primary L + V inclusions hosted along variably healed grain-boundaries within a patch of quartz. b. Secondary electron image of opened type-II inclusions on a partially healed grain-interface. Ca-rich and K-rich solid phases (accidental?) are exposed.

Salt in pore spaces and vugs

Groups of small (1–3 μm) euhedral crystals of halite (identified by SEM–EDS) occur in pore spaces, fractures, and vug-like depressions in all mineral phases (Fig. 6). The abundance of these crystals does not appear to correlate with proximity to ore. Using image analysis software (Scion Image®) applied to exposed fracture surfaces in the matrix of Sudbury Breccia photographed by SEM, the total bulk-rock abundance of the halite crystals was estimated to be extremely low (less than 0.001 vol.%). However, the presence of rare clusters of halite crystals may contribute significantly to the soluble halogen budget in the matrix of the breccia (see below).

CHLORINE AND BROMINE CONTENTS OF THE BULK ROCK

Concentrations of Cl and Br in Sudbury Breccia matrix are listed in Table 1. Figure 7 is a log–log plot of the bulk Br *versus* Cl concentrations in the matrix of the Sudbury Breccia. From this diagram, it is evident that peripheral and proximal samples are significantly enriched in bulk Cl (1.5–10 times higher) and Br (1.5–2 times higher) relative to distal samples. The enrichment in bulk Cl with proximity to ore is consistent with the results of Jago *et al.* (1994) for Sudbury Breccia at the McCreedy East mine. Although the Br contents of peripheral and proximal samples are similar, many proximal samples are enriched in Cl relative to the peripheral samples. The maximum background concentrations or "threshold" values observed in the distal samples were 357 ppm Cl and 3.2 ppm Br. For Cl, this threshold value is higher than the background concentration (250 ppm) observed by Jago *et al.* (1994). Using background values of 357 ppm Cl and 3.2 ppm Br, ~60% of samples in the peripheral division and the proximal division yielded anomalous Cl contents, whereas ~40–50% of the results in these divisions were anomalous with respect to Br.

Figures 8a–b are false-color maps of bulk Cl and Br concentration in the Sudbury Breccia matrix from the proximal and peripheral sample sites in the Fraser Copper Zone generated using the software package Surfer®. The software used a kriging algorithm to interpolate concentration gradients between adjacent sample points, with the area of influence equal to one half of the distance between adjacent samples. The transitions between maximum background and anomalous concentrations for Cl and Br are labeled as the "threshold concentration". This threshold is indicated on all contour plots at the blue–green transition in the color contouring. Note that elevated concentrations of Cl and Br appear to be related spatially to the most intensely brecciated portion of the underground study-area (Fig. 2b); the main zone of breccia adjacent to Zones 37 and 38 contains approximately 46 vol.% Sudbury Breccia (matrix and clasts), whereas the adjacent hanging-wall of this zone of Sudbury Breccia is comparatively weakly brecciated, containing less than 18 vol.% matrix and clasts (Fedorowich *et al.* 1999). The limits of this zone of breccia to the east of the haulage drift between Zones 38 and 37 and in the hanging wall of Zone 38 are unknown owing to the scarcity of drilling data in that area (D. King, pers. commun., 2002).

The diagonal lines in Figure 7 are lines of constant bulk Cl:Br ratio. The bulk Cl:Br ratios in the distal samples range from 71 to 166. Bulk Cl:Br ratios in the peripheral division are similar (79 to 230). Bulk Cl:Br ratios in the proximal division are much more variable than in distal and peripheral samples, ranging from 46 to 581. In general, the bulk Cl:Br ratio increases with increasing proximity to ore.

CHLORINE AND BROMINE CONTENTS (WATER-SOLUBLE AT 20°C)

Results of partial analyses (not all anions and cations were measured) of leachates are listed in Table 2. Concentrations of cations and anions in the leachate solutions are expressed in μg/g (ppm) of rock powder to allow a simple comparison of bulk rock and leachate data. The leachate compositions represent the concentration of (water) soluble Cl (as Cl^-), Br (as Br^-), and other ions in the bulk rock. Figure 9 is a log–log plot of the soluble Br *versus* Cl concentrations in the leachates. Concentrations of soluble Cl in the leachates range from 74 ppm to 120 ppm in distal samples, 40 to 454 ppm in peripheral samples, and 122 to 372 ppm in proximal samples. Soluble Cl accounts for between ~6.4 and 70.6% of the total (bulk) Cl present in the matrix of the Sudbury Breccia, and on average, accounts for ~35 to 40% of the total Cl in peripheral and distal samples. Interestingly, soluble Cl contributes the least to the bulk-rock Cl content in samples from the proximal division (mean 13.9%, range 6.4–27.5), where bulk Cl contents are the highest. The presence of insoluble chlorine-bearing minerals accounts for the lower fractions of soluble Cl noted in some of the proximal and peripheral breccias that are anomalous with respect to bulk-rock Cl, but not soluble Cl.

Concentrations of soluble Br range from 0.03 to 0.79 ppm in distal samples, 0.07 to 3.72 ppm in peripheral samples, and 0.10 to 3.32 ppm in proximal samples. The amount of soluble Br as a percentage of the bulk-rock Br is similar in all sample divisions, ranging from 9.2 to 88.2%, averaging 25–35%. More than 85% of the breccia samples analyzed contain less than 50% soluble Br, the remainder of which must be trapped in insoluble minerals. In general, the majority of peripheral and proximal samples have higher soluble Br and Cl con-

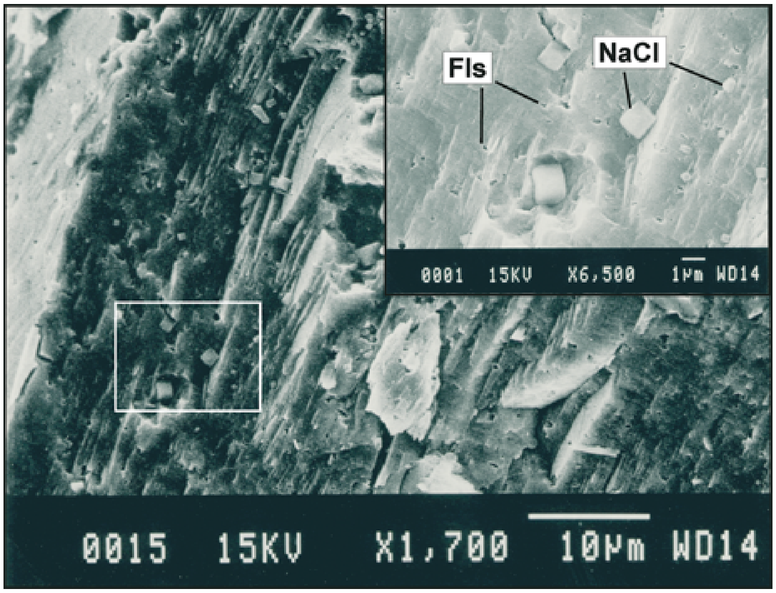

FIG. 6. Secondary electron images of salt (NaCl) crystals occurring on a pitted fracture-surface in feldspar from the matrix of Sudbury Breccia. Note that the crystals are not spatially associated with fluid inclusions (FIs; inset image; enlargement of boxed area). Rather, they appear to be dispersed over the entire fracture-surface. Fluid inclusions are very small in comparison to the salt crystals.

TABLE 1. LEVELS OF CONCENTRATION OF Cl AND Br IN SAMPLES OF SUDBURY BRECCIA MATRIX, FRASER COPPER ZONE, STRATHCONA EMBAYMENT, SUDBURY, ONTARIO

Sample #	(2) Class	Cl	Br	Cl:Br
NRD60-1	distal	228.6	1.6	139.8
NRD60-2	distal	180.9	1.8	99.4
NRD60-4	distal	200.0	1.5	133.3
NRD60-5	distal	226.8	3.2	70.9
NRD60-6	distal	257.5	2.9	88.1
OD49081-1	distal	272.7	2.2	124.7
OD49081-2	distal	357.2	2.3	156.7
OD49081-3	distal	317.9	1.9	166.3
(1) mean (1σ)	*n* – 8	255.2	2.2	122.4
		(55.6)	(0.6)	(31.4)
B2 M0-1	proximal	1203.0	4.9	245.5
B2 M5-1	proximal	1682.3	5.4	311.5
B2 M10-2	proximal	1989.4	5.6	355.3
B2 M17-1	proximal	1352.1	5.3	255.1
SE M0	proximal	1336.3	4.2	318.2
SE M5	proximal	1917.3	3.3	581.0
SE M10	proximal	1559.7	2.8	557.0
SE M15	proximal	1785.0	4.1	435.4
SE M20	proximal	1267.1	6.4	198.0
SE M25	proximal	931.0	2.7	344.8
B2 M20-1	proximal	527.8	3.5	150.8
B2 M25-1	proximal	431.1	3.2	134.7
B2 M30-1	proximal	756.1	2.9	260.7
JHO-T	proximal	744.7	5.2	143.2
SE M30	proximal	790.7	3.1	255.1
NE M-5	proximal	302.1	3.3	91.5
NE M0	proximal	371.6	3.6	103.2
JHO-2	proximal	168.2	3.7	45.5
JHO-16	proximal	262.2	3.4	77.1
C16	proximal	457.1	3.9	117.2
NE M5	proximal	610.1	4.2	145.3
NE M10	proximal	920.4	4.2	219.1
NE M15	proximal	526.1	3.0	175.4
NE M20	proximal	527.5	4.6	114.7
JHO-Q4	proximal	1203.3	4.4	273.5
mean (1σ)	*n* = 25	944.9	4.0	236.4
		(539.2)	(1.0)	(137.4)
NE M65	peripheral	315.5	3.4	92.8
NE M75	peripheral	304.6	2.2	138.5
M86 SE	peripheral	338.6	3.1	109.2
M210 SE	peripheral	190.6	2.4	79.4
NE M40	peripheral	317.0	3.1	102.3
NE M45	peripheral	347.0	2.9	119.7
NE M50	peripheral	290.8	3.2	90.9
NE-4	peripheral	289.5	3.2	90.5
NE-11	peripheral	310.2	2.7	114.9
NE18	peripheral	261.7	2.4	109.0
M203 SE	peripheral	191.3	2.0	95.7
SE M35	peripheral	823.7	4.0	205.9
SE M40	peripheral	609.8	4.1	148.7
SE M45	peripheral	703.8	4.3	163.7
M50 SE	peripheral	788.1	4.8	164.2
M60 SE	peripheral	661.1	4.4	150.3
M71 SE	peripheral	708.7	4.9	144.6
M106 SE	peripheral	415.5	3.5	118.7
M115 SE	peripheral	463.7	3.4	136.4
M142 SE	peripheral	658.3	5.2	126.6
M152 SE	peripheral	583.7	4.3	135.7
M163 SE	peripheral	641.6	4.8	133.7
M173 SE	peripheral	551.9	4.4	125.4
M177 SE	peripheral	621.1	4.8	129.4
M184 SE	peripheral	424.4	3.2	132.6
M194 SE	peripheral	661.9	4.7	140.8
M233 SE	peripheral	537.0	3.1	173.2
M259 SE	peripheral	438.5	3.5	125.3
M267 SE	peripheral	614.0	3.7	165.9
NE M30	peripheral	377.3	2.8	134.8
NE M55	peripheral	412.5	4.0	103.1
NE M60	peripheral	528.2	5.1	103.6
NE-3	peripheral	689.6	5.1	135.2
NE-6	peripheral	513.1	4.4	116.6
NE-7	peripheral	428.7	3.9	109.9
NE-8	peripheral	401.6	3.1	129.5
NE-9	peripheral	558.6	4.1	136.2
NE-10	peripheral	712.8	3.1	229.9
NE-17	peripheral	619.3	4.6	134.6
NE14	peripheral	395.8	3.6	109.9
NE-15	peripheral	587.8	4.0	147.0
NE19	peripheral	403.5	3.6	112.1
NE20	peripheral	539.0	3.1	173.9
NE21	peripheral	495.4	3.0	165.1
M220 SE	peripheral	386.7	3.4	113.7
M228 SE	peripheral	1075.4	4.9	219.5
37-240-1	peripheral	451.2	2.0	225.3
37-240-3	peripheral	467.3	4.4	106.3
37-240-5	peripheral	287.6	3.1	92.5
37-240-6	peripheral	346.5	3.1	111.5
37-240-7	peripheral	386.6	3.7	105.7
37-240-8	peripheral	438.9	3.3	133.3
37-240-10	peripheral	299.2	2.6	113.0
37-240-11	peripheral	316.3	3.8	82.3
37-240-12	peripheral	277.2	3.1	89.2
mean (1σ)	*n* – 55	481.1	3.7	130.9
		(174.2)	(0.8)	(34.0)

The concentration of Cl and Br is quoted in ppm. (1) Mean of *n* analyses (one standard deviation on the mean). (2) Class of sample: proximal (<10 m from ore), peripheral (10 150 m from ore), distal (>150 m from ore).

tents than distal samples, suggesting that soluble Br and Cl contents increase with proximity to ore. The concentrations of soluble Cl and Br are well correlated.

Also plotted with the leachate data is the range in Cl:Br ratios from modern saline and briney groundwaters from the Fraser mine (Frape & Fritz 1987), and the estimated composition of the parental briney groundwater for the Canadian Shield at Sudbury (Pearson 1985). The ratio Cl:Br in the leachates ranges from 83 to 309, and shows no systematic variation with proximity to ore. Although many of the leachates have a Cl:Br ratio very close to or within the range for groundwater compositions, a significant number of leachates have an unusually high Cl:Br ratio and have been influenced by some other fluid source or process (see below).

SULFATE CONTENT (WATER-SOLUBLE AT 20°C)

Some leachates from proximal and peripheral samples yielded anomalously high concentrations of SO_4^{2-} relative to distal samples (Table 2). Sulfate contents obtained from proximal and peripheral samples range from 0.4 to 95.6 ppm, whereas distal samples yielded between 0.2 and 2.6 ppm. Many leachates from proximal and peripheral samples show enrichment in soluble SO_4^{2-}. There is no correlation between the soluble SO_4^{2-} and Cl, or SO_4^{2-} and Br abundances in the leachates. Data for bulk SO_4^{2-} were not obtained. Therefore, it is uncertain whether anomalous sulfate contents in leachates from peripheral and proximal samples are linked to higher contents of sulfate in trapped fluids near the ore. A possible source of sulfate in our samples is the oxidation of very small amounts of disseminated sulfide (*i.e.*, chalcopyrite) in the matrix of the breccia. It is interesting to note that although Frape & Fritz (1987) found SO_4^{2-} in most groundwaters from the Canadian Shield, they found that the Fraser mine groundwaters contained locally elevated concentrations of SO_4^{2-}, possibly from the oxidation of sulfide minerals.

DISCUSSION

Changes in halogen content with proximity to ore

By subtraction of the soluble fraction of Cl and Br from the bulk concentrations obtained by XRF for those samples that were leached, the Cl and Br content and Cl:Br ratios in the insoluble fractions (residues, after leaching) were determined (Table 2). On a log–log plot of Br *versus* Cl concentration in the insoluble fraction (Fig. 10), the increase in Cl:Br ratio with increasing proximity to ore is much exaggerated compared to a similar plot for bulk (soluble + insoluble) Cl and Br (Fig. 7). Calculated Cl:Br ratios in the insoluble fraction range from 48 to 811, with proximal samples all exhibiting very high Cl:Br ratios (mean = 493). Therefore, the insoluble mineral constituents control the bulk Cl:Br ratio of the matrix, despite the large soluble component of the total halogen budget.

Hanley & Mungall (2003) demonstrated that the modal abundance and Cl content of the principal Cl-bearing minerals (amphibole, chlorite, epidote) in the matrix of the Sudbury Breccia increases as footwall mineralization is approached. The highest abundances of Cl-bearing insoluble minerals and highest Cl contents within those minerals were observed in proximal samples. The growth of large volumes of these minerals in the vicinity of footwall-style mineralization was found to be related to retrograde metamorphic reactions, which overprinted the contact-metamorphic aureole of the SIC only in ore-bearing zones of Sudbury Breccia (Hanley & Mungall 2003). The relatively large ionic radius of bromine makes it unlikely that there is any marked replacement of the OH^- group in hydroxysilicates by Br^- (*e.g.*, Correns 1956). Therefore, during growth of hydroxysilicates, the incorporation of Cl^- into the OH^- site is favored over Br. By this process, the

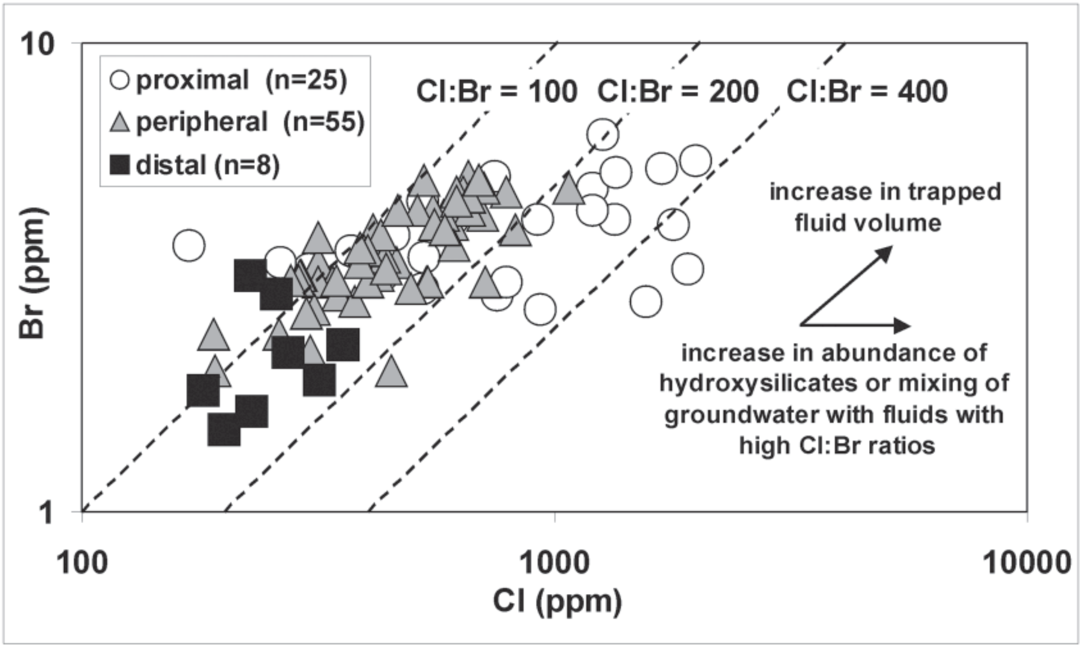

FIG. 7. Log–log plot of bulk-rock Br *versus* Cl in Sudbury Breccia matrix samples. Diagonal lines are labeled with a constant Cl:Br ratio. Increasing Cl with no corresponding increase in Br suggests increasing abundances of hydroxysilicate minerals, which preferentially concentrate Cl, or increasing Cl:Br ratio in trapped fluids (notable in the peripheral to proximal transition). Increasing Cl and Br suggest increasing abundance of trapped fluids (notable in the distal-to-peripheral transition).

TABLE 2. COMPOSITION OF AQUEOUS LEACHATES, BULK WATER CONTENT, AND INSOLUBLE RESIDUES DERIVED FROM SUDBURY BRECCIA MATRIX, FRASER COPPER ZONE, STRATHCONA EMBAYMENT, SUDBURY, ONTARIO

		aqueous leachate										insoluble fraction			(4) % soluble of total		
Sample #	(2)Class	Na^+ (3) µg/g	K^+ µg/g	Mg^{2+} µg/g	Ca^{2+} µg/g	Ca: Mg	Ca: Na	Na: K	Cl^- µg/g	Br^- µg/g	SO_4^{2-} µg/g	Cl: Br	Cl ppm	Br ppm	Cl: Br	Cl %	Br %
NEm40	peripheral	89.9	92.8	3.8	45.9	12.2	0.5	1.0	39.8	0.4	9.8	105.7	277.2	2.7	101.8	12.5	12.1
SEm152	peripheral	280.4	36.9	19.5	192.0	9.9	0.7	7.6	391.2	1.7	7.4	231.4	192.5	2.6	73.8	67.0	39.3
NEm65	peripheral	175.8	51.5	9.2	73.0	7.9	0.4	3.4	189.2	0.7	13.2	252.3	126.3	2.7	47.7	60.0	22.1
NEm75	peripheral	123.9	162.1	7.0	61.9	8.9	0.5	0.8	99.1	0.3	15.2	308.6	205.5	1.9	109.4	32.5	14.6
NEm50	peripheral	188.2	67.9	8.3	109.9	13.3	0.6	2.8	93.9	0.9	12.0	106.0	196.9	2.3	85.1	32.3	27.7
NEm45	peripheral	131.1	116.4	6.1	58.7	9.6	0.4	1.1	161.2	0.6	16.8	269.2	185.8	2.3	80.7	46.5	20.6
SEm228	peripheral	133.1	11.1	23.4	364.7	15.6	2.7	12.0	328.1	2.7	12.2	120.3	747.3	2.2	344.1	30.5	55.7
SEm45	peripheral	192.8	60.5	10.3	95.4	9.2	0.5	3.2	186.9	0.8	3.9	245.5	516.9	3.5	146.1	26.6	17.7
SEm267	peripheral	163.2	33.1	12.8	161.5	12.6	1.0	4.9	187.7	1.1	6.6	167.8	426.3	2.6	165.2	30.6	30.2
SEm233	peripheral	277.6	68.4	18.1	103.3	5.7	0.4	4.1	257.7	1.1	1.8	241.9	279.3	2.0	137.3	48.0	34.4
NE-21	peripheral	230.1	96.3	12.6	163.3	12.9	0.7	2.4	180.3	0.9	2.0	200.0	315.1	2.1	150.2	36.4	30.0
NE-3	peripheral	221.4	25.3	14.5	283.1	19.5	1.3	8.8	384.1	2.1	6.0	184.1	305.5	3.0	101.4	55.7	40.9
SEm86	peripheral	264.0	34.4	13.7	31.8	2.3	0.1	7.7	175.7	0.9	0.5	191.7	162.9	2.2	74.6	51.9	29.6
SEm210	peripheral	95.3	35.3	7.2	52.1	7.2	0.5	2.7	89.4	0.8	0.7	110.0	101.2	1.6	63.8	46.9	33.9
SEm173	peripheral	129.5	18.7	4.4	67.6	15.3	0.5	6.9	152.1	1.4	2.2	105.1	399.8	3.0	135.4	27.6	32.9
NE-7	peripheral	134.9	18.9	10.9	105.8	9.7	0.8	7.1	181.2	1.4	2.0	132.2	247.5	2.5	97.9	42.3	35.1
SEm163	peripheral	116.0	30.1	5.8	133.1	23.1	1.1	3.9	190.3	1.6	1.1	118.1	451.3	3.2	141.5	29.7	33.6
37-240-1	peripheral	205.2	322.7	15.2	70.7	4.6	0.3	0.6	79.1	0.5	3.2	170.0	491.8	4.6	107.5	13.9	9.2
37-240-2	peripheral	359.8	344.7	32.7	129.7	4.0	0.4	1.0	268.8	1.8	2.1	152.1	182.4	0.2	772.5	59.6	88.2
SEm194	peripheral	146.4	32.6	14.3	153.1	10.7	1.0	4.5	219.1	1.4	2.5	160.5	442.8	3.3	132.8	33.1	29.0
37-240-4	peripheral	333.3	65.5	34.6	219.2	6.3	0.7	5.1	453.5	3.7	0.4	121.9	189.1	3.8	49.7	70.6	49.4
NE-10	peripheral	118.9	24.7	15.0	108.7	7.2	0.9	4.8	107.4	0.6	1.1	173.7	605.4	2.5	243.9	15.1	19.9
SEm115	peripheral	109.8	32.2	3.1	134.5	42.7	1.2	3.4	316.0	1.0	1.9	301.2	147.7	2.4	62.8	68.1	30.9
(1) mean	*n* = 23	183.5	77.5	13.2	126.9	11.8	0.8	4.3	205.7	1.2	5.4	181.3	312.9	2.6	148.9	40.7	32.1
(1σ)		(74.9)	(86.6)	(8.1)	(77.8)	(8.2)	(0.5)	(2.9)	(106.4)	(0.8)	(5.1)	(63.1)	(165.3)	(0.8)	(147.7)	(16.9)	(16.2)
SEm5	proximal	120.4	18.8	12.4	123.0	9.9	1.0	6.4	122.4	0.7	28.4	179.7	1794.9	2.6	685.4	6.4	20.6
B2m5	proximal	419.2	234.7	17.2	245.5	14.3	0.6	1.8	198.6	2.2	95.6	90.8	1483.7	3.2	461.9	11.8	40.5
SEm10	proximal	246.7	75.8	10.5	120.0	11.5	0.5	3.3	159.4	1.1	50.4	148.4	1400.3	1.7	811.3	10.2	38.4
JHO-QSX	proximal	106.0	60.6	7.2	90.4	12.6	0.9	1.7	111.4	0.9	44.4	127.3	1091.9	3.5	309.8	9.3	19.9
SEm20	proximal	120.8	53.8	10.1	263.3	26.2	2.2	2.2	218.4	1.8	5.4	122.6	1048.7	4.6	227.1	17.2	27.8
B2m0	proximal	124.9	74.8	10.4	193.4	18.7	1.5	1.7	185.8	1.4	4.9	130.3	1017.2	3.5	292.8	15.4	29.1
B2m17	proximal	217.2	74.0	14.4	289.3	20.1	1.3	2.9	371.9	3.3	1.6	112.2	980.2	2.0	494.0	27.5	62.6
SEm25	proximal	104.9	66.4	10.0	109.0	10.9	1.0	1.6	122.6	1.5	3.1	83.2	808.4	1.2	659.6	13.2	54.6
mean (1σ)	*n* = 8	182.5	82.4	11.5	179.2	15.5	1.1	2.7	186.3	1.6	29.3	124.3	1203.2	2.8	492.7	13.9	36.7
		(102.6)	(60.2)	(2.9)	(73.6)	(5.3)	(0.5)	(1.5)	(79.1)	(0.8)	(31.0)	(28.9)	(304.9)	(1.1)	(197.3)	(6.1)	(14.5)
OD49-1	distal	172.7	192.3	10.0	48.2	4.8	0.3	0.9	77.8	0.5	2.4	171.7	194.9	1.7	112.4	28.5	20.7
OD49-2	distal	186.4	208.7	11.8	80.4	6.8	0.4	0.9	101.5	0.7	1.4	141.6	255.7	1.6	163.7	28.4	31.5
OD49-3	distal	286.6	399.7	14.0	64.9	4.6	0.2	0.7	73.5	0.4	2.6	207.4	244.4	1.6	157.0	23.1	18.5
NRD60-1	distal	233.0	113.7	12.4	90.7	7.3	0.4	2.0	103.4	0.3	1.9	295.6	125.2	1.3	97.4	45.2	21.4
NRD60-6	distal	288.9	45.9	28.3	79.3	2.8	0.3	1.3	119.6	0.8	0.2	152.0	137.9	2.1	64.5	46.4	26.9
mean (1σ)	*n* = 5	233.5	192.0	15.3	72.7	5.3	0.3	1.2	95.1	0.5	1.7	193.7	191.6	1.7	119.0	34.3	23.8
		(48.6)	(119.1)	(6.6)	(14.8)	(1.6)	(0.1)	(0.5)	(17.2)	(0.2)	(0.9)	(55.7)	(53.3)	(0.3)	(37.2)	(9.6)	(4.7)

---

(1) Mean result of *n* analyses (one standard deviation on the mean). (2) Class of sample: proximal (<10 m from ore), peripheral (10–150 m from ore), distal (>150 m from ore). (3) µg of cation or anion per g of pulverized Sudbury Breccia matrix (equivalent to ppm). (4) % soluble Cl and Br determined using results of the whole-rock analyses for leached samples.

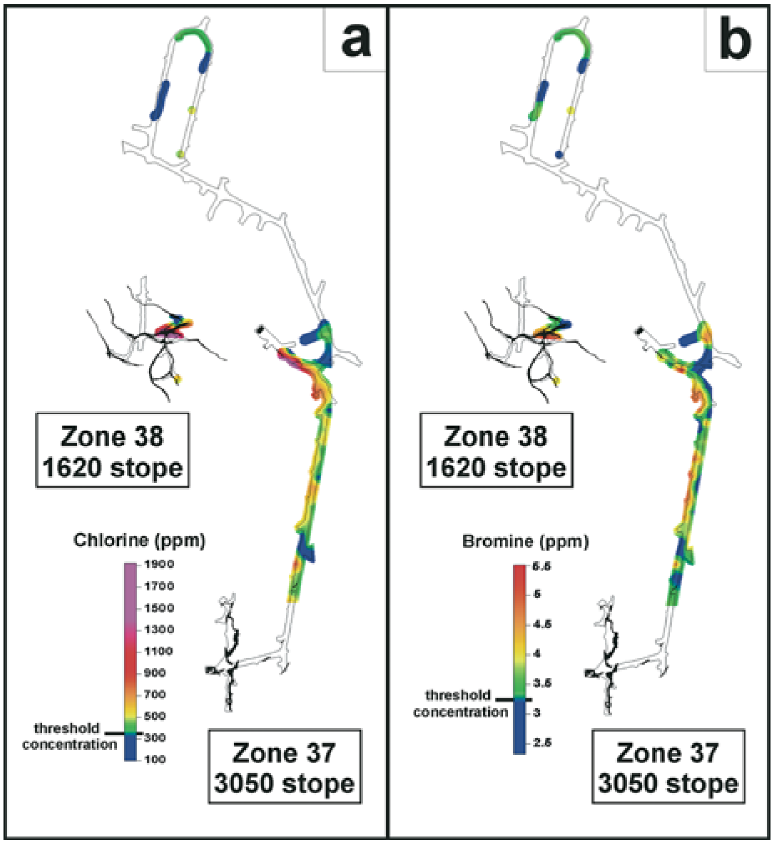

FIG. 8. Distribution of Sudbury Breccia, bulk Cl, and Br in the underground study-area. a. Distribution of bulk-rock Cl in the Sudbury Breccia matrix. b. Distribution of bulk-rock Br in the Sudbury Breccia matrix. Note that the highest concentrations of Cl and Br are associated with the most intensely brecciated portion of the ore-bearing breccia zone (see Fig. 2b).

growth of large volumes of mineral phases excluding Br will effectively enrich the bulk rock in Cl over Br. We suggest that this process explains the increase in bulk Cl:Br ratio with proximity to ore. Such a process may be *independent* of changes in the Cl:Br ratio of the ambient fluids, and entirely *unrelated* to any changes in their total salinity. In this study, elevated Cl:Br ratios in the insoluble mineral fraction do not indicate that the equilibrating fluids that supplied halogens to the crystallizing phases had unusually high Cl:Br ratios.

The concentrations of soluble Cl and Br in the matrix of the Sudbury Breccia demonstrate positive correlations with proximity to ore and with bulk abundance of halogens. There is no correlation between leachable Cl:Br ratio and proximity to ore; however, the range in Cl:Br ratios observed in the leachates is wide, considering the generally conservative nature of this ratio and the narrow range of Cl:Br ratios expressed by fluids from single sources (*e.g.*, the Sudbury groundwaters). The range of Cl:Br ratios in the leachates cannot reflect the entrapment of a single fluid in the dominant population of fluid inclusions (those of type II).

Variations in relative concentrations of cations

Figure 11 shows the concentrations of the major cations in the leachates (Ca^{2+}, Na^+, and K^+). Also plotted is the field of saline and briney groundwater compositions from the Fraser mine (Frape & Fritz 1982) and fluid compositions occurring in primary inclusions within sulfide minerals from the Fraser Cu Zone (Farrow 1994). Leachate compositions show a trend from Ca-poor with high and variable Na and K content (distal samples, and some of the peripheral samples) to Ca-rich with a low and narrow Na and K content overlapping with the groundwater and sulfide-hosted fluid compositions. Cation–cation ratios (*e.g.*, Ca:Na) vary widely in the leachates. If the Ca:Na ratios are compared to the

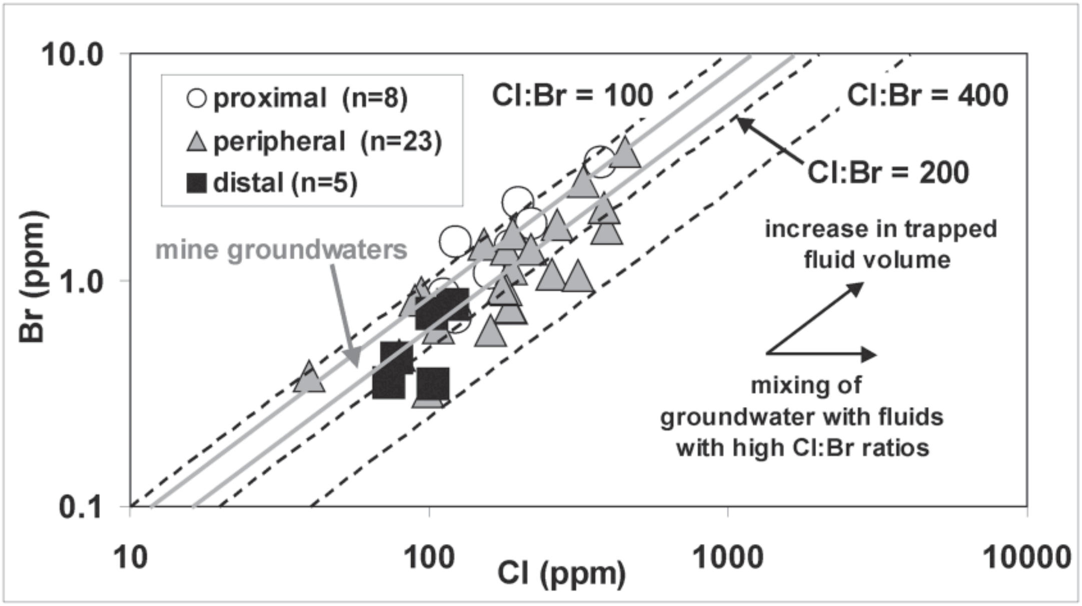

FIG. 9. Log–log plot of water-soluble Br (as Br$^-$) *versus* Cl (as Cl$^-$) in matrix leachates. Dashed lines are labeled with a constant Cl:Br ratio. Grey region indicates Cl:Br ratios for saline and briney groundwaters (Frape & Fritz 1982). In general, proximal and peripheral samples have higher soluble Cl and Br contents than distal samples. The range in Cl:Br ratios is too wide to be the result of trapped groundwaters alone.

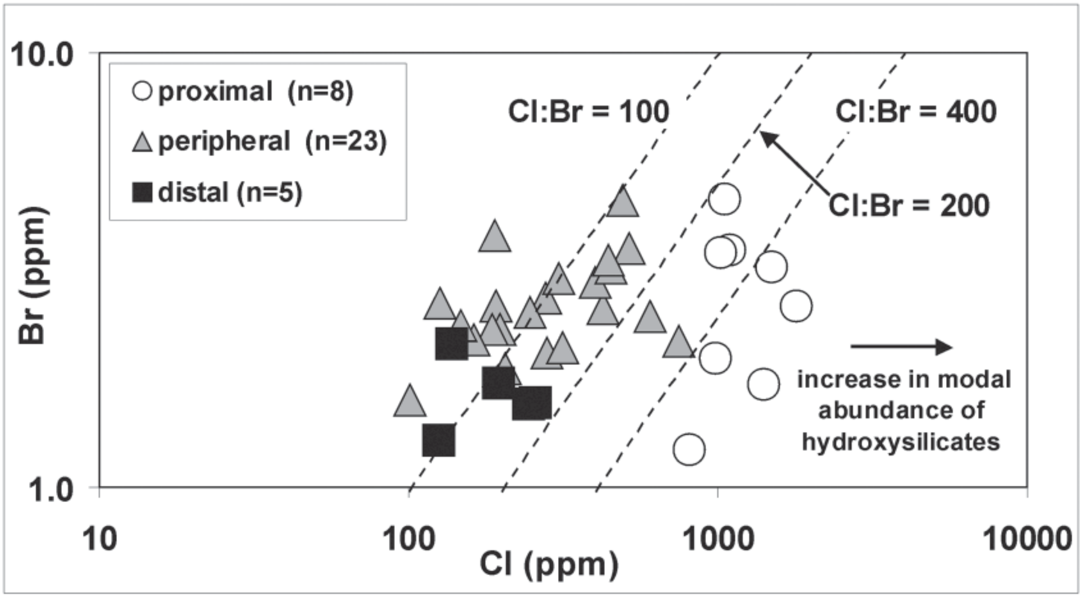

FIG. 10. Log–log plot of calculated Br *versus* Cl in the insoluble residue (after leaching). Cl:Br ratios increase with proximity to ore, and are very high in many of the proximal samples. Independent of the soluble halogens in the matrix, the Cl content and abundance of insoluble silicates are the principal controls on the bulk Cl:Br ratio in the matrix. Only a slight increase in the Br content within the insoluble fraction is noted with increasing proximity to ore.

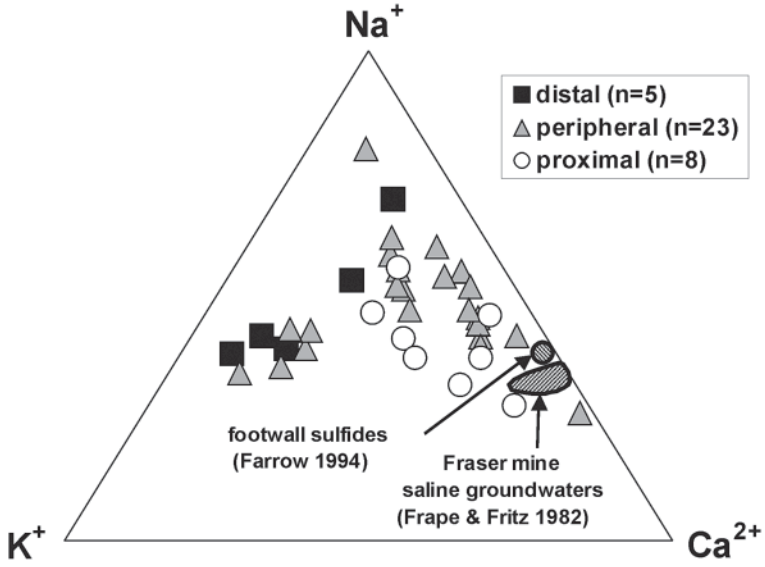

FIG. 11. Diagram showing the speciation of major cations Na$^+$, K$^+$, and Ca^{2+} in the leachates. Compositions span a range from Na–K-dominant fluid to Ca-dominant fluid whose relative speciation overlaps with compositions of modern groundwater (Frape & Fritz 1982) and the composition of fluids trapped in sulfide minerals from the footwall ore-zones (Farrow 1994).

Cl:Br ratios in the leachates (Fig. 12), the presence of halogens from several different sources is confirmed. Those leachates with increasing Ca:Na ratio that trend toward the groundwater field in Figure 12 exhibit a lowering and narrowing of the range in Cl:Br ratios. Leachates exhibiting the highest Ca:Na ratios have Cl:Br ratios that overlap with groundwater compositions. The trend of decreasing Cl:Br ratios with increasing Ca:Na is bimodal in nature, with two separate populations of leachate visible in Figure 12 (labeled trends 1 and 2).

We propose that the variable Cl:Br and Ca:Na ratios expressed by the leachates may reflect (i) the presence of very small amounts of halite (Fig. 6) deposited by early, halite-saturated parental groundwaters typical of the Canadian Shield, or (ii) the entrapment of hybrid (mixed) fluids (in type-II inclusions) derived from mixing of Ca-rich parental groundwater with fluids of possibly magmatic origin that had low Ca:Na (or Ca:K) ratios and highly variable Cl:Br ratios.

Evidence for halite deposition

The origin of the leachates with very high Cl:Br and low Ca:Na ratios (trend 1, Fig. 12) may be explained by the addition of halite (*not* in fluid inclusions) to the matrix of the Sudbury Breccia. To visualize this possibility, a model curve was calculated (Fig. 13) to represent the leachate composition in terms of its Ca:Na and Cl:Br ratio changing as a function of the halite abundance in the matrix. For the model curve, the equation used to calculate the theoretical Cl:Br ratio in the soluble halogen fraction of a Sudbury Breccia sample containing contributions from both groundwater-bearing, type-II fluid inclusions and halite is:

$$\left(\frac{Cl}{Br}\right)_{leachate} = \frac{[Cl]^{matrix}_{halite} + [Cl]^{matrix}_{groundwater}}{[Br]^{matrix}_{halite} + [Br]^{matrix}_{groundwater}}$$

where $[Cl]^{matrix}_{halite}$ and $[Br]^{matrix}_{halite}$ are the concentrations of Cl and Br (in µg/g) in the matrix of the sample due to the presence of halite, and $[Cl]^{matrix}_{groundwater}$ and $[Br]^{matrix}_{groundwater}$ are the concentrations of Cl and Br in the matrix resulting from the presence of trapped groundwater. The terms $[Cl]^{matrix}_{halite}$ and $[Br]^{matrix}_{halite}$, involving the halite contribution, were calculated by multiplying the concentrations of Cl and Br in halite by the wt% abundance of halite in the matrix, which varied from 10^{-8} to 10^{-5} wt%, to produce the model curve. The concentrations of Br and Cl in halite were fixed at 5000 ppm and 601,200 ppm, respectively. The Br concentration was chosen as typical of terrestrial halite, and in agreement with partitioning experiments for Br between halite and brine solutions indicating that the Br content

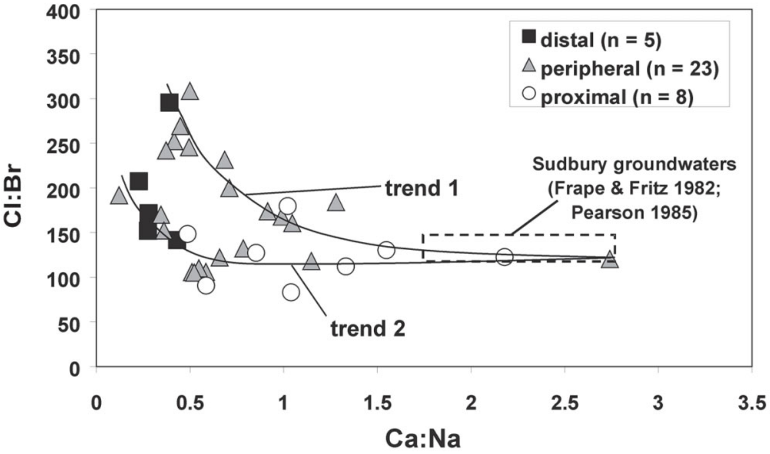

FIG. 12. Plot of Cl:Br ratio *versus* Ca:Na ratio in the leachates. A decrease and narrowing of the range in Cl:Br ratios are correlated with increasing Ca:Na ratio. Groundwater compositions for the study area fall into area represented by the dashed box and are taken from Frape & Fritz (1982) and Pearson (1985). The scatter in Cl:Br ratio for leachates with low Ca:Na ratio may be fitted by at least two compositional trends (labeled trends 1 and 2).

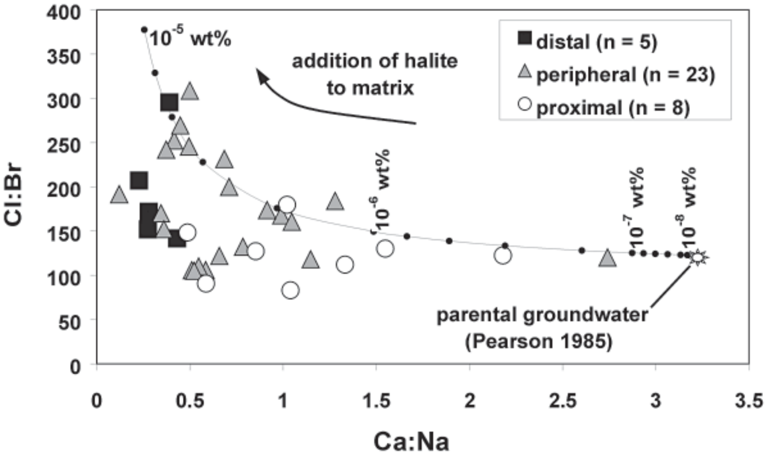

FIG. 13. Model curve resulting from the deposition of increasing amounts of halite (from 10^{-8} wt% to 10^{-5} wt%) in the matrix of the Sudbury Breccia, which already contains 10^{-5} wt% trapped groundwater in fluid inclusions. The addition of halite can explain the range in Ca:Na ratios observed in the leachates, but can only account for a single compositional trend (trend 1) assuming that the Cl:Br ratio of the halite added to the matrix is constant.

of very small amounts of precipitated halite relative to the volume of the source brine tend to be high (Siemann & Schramm 2000). The exact Br content of the halite is not known. However, order-of-magnitude changes in Br concentration in the halite result in only negligible changes in the curvature of the resulting model curve. The Cl content of halite was fixed at the stoichiometric value for pure halite (606,200) less the concentration of Br (5000 ppm), which would be substituting for Cl, or 601,200 ppm. For the groundwater contribution, the terms $[\mathrm{Cl}]^{matrix}_{groundwater}$ and $[\mathrm{Br}]^{matrix}_{groundwater}$ were calculated by multiplying the concentrations of Cl

(270,000 ppm) and Br (2200 ppm) in the parental groundwater for the Sudbury area (Pearson 1985) by the wt% abundance of this fluid in the matrix (10^{-5} wt%). This fluid volume was determined by gas chromatographic analysis of the water released from crushed samples of Sudbury Breccia matrix by Hanley (2002). The composition of the parental groundwater chosen represents the composition of the most saline (halite-saturated) groundwater composition that exists below a depth of 1700 m in the study area (Pearson 1985, Gascoyne *et al.* 1987). Since the paleodepth of formation for the footwall ores, and of alteration and metamorphism of the Sudbury Breccia in the underground study area, is estimated to be well below the depth at which the parental groundwater occurs (*i.e.*, between 3000 and 5000 m; Molnár *et al.* 2001, Hanley & Mungall 2003), the groundwater trapped in type-II inclusions along recrystallized grain margins should be most comparable to the parental groundwater (*i.e.*, most saline) in its composition.

Similarly, the equation used to calculate the Ca:Na ratio for the model curve is:

$$\left(\frac{Ca}{Na}\right)_{leachate} = \frac{[Ca]^{matrix}_{groundwater}}{[Na]^{matrix}_{halite} + [Na]^{matrix}_{groundwater}}$$

where $[\mathrm{Na}]^{matrix}_{halite}$ is the concentration of Na (in ppm) in the matrix of the sample due to the presence of halite (the Ca content of halite is assumed to be negligible), and $[\mathrm{Ca}]^{matrix}_{groundwater}$ and $[\mathrm{Na}]^{matrix}_{groundwater}$ are the concentrations of Ca and Na in the matrix resulting from the presence of trapped groundwater. As for the halogens, the $[\mathrm{Na}]^{matrix}_{halite}$ term was calculated by multiplying the concentrations of Na in halite by the wt% abundance of halite in the matrix, which was varied from 10^{-8} to 10^{-5} wt% to produce the model curve. The Na concentration in halite was fixed at 393800 ppm (stoichiometric, pure halite). Similarly, for the groundwater contribution, the terms $[\mathrm{Ca}]^{matrix}_{groundwater}$ and $[\mathrm{Na}]^{matrix}_{groundwater}$ were calculated by multiplying the concentrations of Ca (109,000 ppm) and Na (34,000 ppm) in the parental groundwater for the Sudbury area (Pearson 1985) by the wt% abundance of this fluid in the matrix (10^{-5} wt%).

In Figure 13, the resulting model curve fits a significant portion of the leachate data. Samples that yielded leachates with low Ca:Na ratios, and Cl:Br ratios significantly above that of the parental groundwater, represent matrix samples that contain up to $\sim 8 \times 10^{-5}$ wt% halite in addition to their groundwater component. Halite contributions to the leachate begin to significantly raise the Cl:Br ratio in the leachate as halite abundance reaches $\sim 10^{-6}$ wt%. Samples containing less than $\sim 10^{-6}$ wt% halite generated leachates that are indistinguishable from the parental groundwater with respect to their Cl:Br ratios, but express lower Ca:Na ratios.

Halite deposition in the matrix of Sudbury Breccia is supported by the observation of *accidentally* trapped salt crystals in pore spaces and vugs. They are presumably a feature common to the crystalline rocks of the Canadian Shield and demonstrate that the ancient brines were halite-saturated at depth during their early history (Pearson 1985). For example, Guha & Kanwar (1987) reported similar vugs containing halite crystals in deep crystalline rocks at the Copper Rand mine, Chibougamau, Quebec. The structures that the salt crystals now occupy (Figs. 6a–b) could not have existed as open structures after salt deposition, since the modern saline and briney groundwaters in the underground study-area are undersaturated with respect to halite and would therefore dissolve any pre-existing halite with which they would come into contact. The salt crystals cannot be related to the occurrence of type-I or type-II fluid inclusions, as they commonly occur in vug-like depressions exposed on fractured surfaces that are entirely devoid of fluid inclusions. It is also most unlikely that the salts are "quench" features resulting from precipitation of trapped fluid upon opening of fluid inclusions, as the halite crystals are invariably euhedral in habit. These are in contrast to the anhedral nature of decrepitation mounds formed by the precipitation of salts around opened inclusions that contained a salt-rich fluid prior to opening.

In general, the presence of small amounts of precipitated halite in the matrix, and an end-member groundwater component trapped along grain boundaries in the dominant type of fluid inclusion (type II), can account for some of the variation in halogen and associated major cation ratios in the leachates (expressed by trend 1; Fig. 12); however, it cannot account for the leachates with variable (notably lower) Cl:Br ratios but also low Ca:Na ratios (trend 2, Fig. 12).

EVIDENCE FOR MIXING OF MAGMATIC FLUID WITH PARENTAL GROUNDWATER

To account for leachate compositions that do not fall on the halite deposition curve, an alternative model involves the mixing of Ca-rich parental groundwater with pulses of magmatic fluid, and entrapment of the hybrid (mixed) fluids in the matrix of the breccia. A hybrid fluid model is in agreement with the work of Marshall *et al.* (1999), who presented stable isotope evidence for the mixing of groundwater and SIC-derived magmatic fluid from assemblages of alteration minerals occurring along footwall sulfide ore – host-rock contacts. The exsolution of a magmatic fluid phase was also proposed by Molnár *et al.* (2001) on the basis of fluid-inclusion studies.

To model the composition of a hybrid fluid, we suggest that fluids of magmatic lineage derived from the

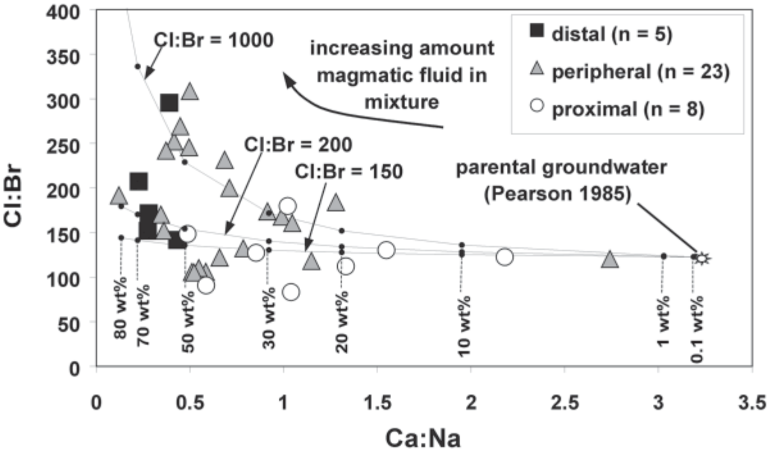

FIG. 14. Model curves resulting from the entrapment of mixtures of groundwater with varying amounts of a fluid with a very low Ca:Na ratio and a variable Cl:Br ratio. In order to explain the range in leachate data, the non-groundwater fluid component in the trapped mixture must make up a significant proportion of the total mixture (up to 80%), and must have exhibited Cl:Br ratios ranging from approximately 100 to over 1000 during its evolution.

SIC were Na- and K-rich brines, with high and variable Cl:Br ratios. Unfortunately, there are no published estimates of the Cl:Br ratio or cation composition for any fluids of magmatic origin associated with the Sudbury Igneous Complex. Molnár *et al.* (2001) reported salinities as high as 60 wt% eq. NaCl in primary inclusions from the footwall environment, which are believed to contain an exsolved magmatic fluid. These inclusions were observed in quartz within granophyric veins considered to represent late-stage magmatic residues of the SIC or partially melted host-rocks. The granophyric veins are composed of quartz, K-feldspar, and very sodic plagioclase. The fluid is believed to have exsolved at ~800°C at a depth of 3–5 km, conditions consistent with thermometry and barometry of the plagioclase–hornblende assemblage in the granophyric veins. Molnár *et al.* (2001) interpreted the low eutectic melting temperatures of the fluid inclusions to be the result of the presence of Ca^{2+}. However, significant concentrations of other cations (Fe, Mn, Ba, Zn, Pb, and K) have been noted in the inclusions, suggesting that Ca^{2+} may not be the dominant cation (in addition to Na^+) responsible for such temperatures of the eutectic (Farrow 1994, Farrow *et al.* 1999, and Molnár *et al.* 2001).

In general, magmatic fluids with a high Cl:Br ratio have been observed consistently in a variety of volcanic and plutonic environments and rock types (Sugiura *et al.* 1963, Basharina 1965, Yoshida *et al.* 1971, Bohlke & Irwin 1992, Snyder & Fehn 2002). For example, *in situ* measurements of "magmatic" waters or geothermal waters in active or recently active volcanic systems indicate that such fluids typically have a high Cl:Br ratio. Early data for fumarolic waters and gases analyzed from a variety of Japanese, Russian, and Indonesian volcanoes present Cl:Br ratios ranging from 200 to over 1000 (Sugiura *et al.* 1963, Basharina 1965, Kraft & Chaigneau 1976). Recent analyses of geothermal waters from crater lakes, fumaroles, and hot springs in the Central American volcanic arc also show consistently very high Cl:Br ratios (range 700–1000) at all sample locations (Snyder & Fehn 2002). Bohlke & Irwin (1992) pointed out that there are problems associated with interpretation of fumarolic data because of the modification of Cl:Br ratios in fluids due to condensation and sublimation of halide phases. This is exemplified in some Japanese volcanoes, where associated chloride sublimates exhibit a wide range of Cl:Br ratios (from 40 to over 2000), with an average ratio lower than the associated fumarolic waters (Yoshida *et al.* 1965). However, these are likely to be reasonable estimates of the true Cl:Br ratio in magmatic water associated with these volcanic systems (Bohlke & Irwin 1992). More recent data (Bohlke & Irwin 1992) show very high Cl:Br ratios, between 1124 and 1235, for primary fluids occurring in fluid inclusions in the Paleozoic St. Austell Granite, an intrusion considered to have originated from partial melting of the lower crust with possible contributions of mantle volatiles (Stone & Exley 1985). Bottrell & Yardley (1988) interpreted the fluid as having exsolved from the crystallizing magma, on the basis of their data on major and trace elements in the inclusions.

On the basis of the studies described above, it is reasonable to assume that fluid of magmatic origin (*i.e.*, an exsolved or degassed aqueous volatile phase) will exhibit variable, but generally *high* Cl:Br ratios. For the purposes of modeling, we hypothesized that aqueous fluids originating from the SIC during its crystallization had similar characteristics to those described above. Three model curves were calculated (Fig. 14) to represent mixing lines between parental groundwater and three magmatic fluids with variable and high Cl:Br ratios. The equations used to calculate the mixing lines are as follows:

$$\left(\frac{Cl}{Br}\right)_{mixedfluid} = \frac{(F\times[Cl]_{magmaticfluid})+((1-F)\times[Cl]_{groundwater})}{(F\times[Br]_{magmaticfluid})+((1-F)\times[Br]_{groundwater})}$$

$$\left(\frac{Ca}{Na}\right)_{mixedfluid} = \frac{[Ca]_{magmaticfluid}}{(F\times[Na]_{magmaticfluid})+((1-F)\times[Na]_{groundwater})}$$

where $[\mathrm{Cl}]_{magmatic\ fluid}$, $[\mathrm{Br}]_{magmatic\ fluid}$, and $[\mathrm{Na}]_{magmatic\ fluid}$ are the concentrations of Cl, Br, and Na (in ppm) in magmatic fluids derived from the SIC. The proposed magmatic fluids contain 50 wt% NaCl (196,900 ppm Na, and 303,100 ppm Cl), no Ca, and have Cl:Br ratios of 150 (Br = 2020.7 ppm), 200 (Br = 1515.5 ppm), and 1000 (Br = 303.1) ppm. The terms $[\mathrm{Cl}]_{groundwater}$, $[\mathrm{Br}]_{groundwater}$, $[\mathrm{Ca}]_{groundwater}$ and $[\mathrm{Na}]_{groundwater}$ are the concentrations of Cl, Br, Ca, and Na (in ppm) in the parental groundwater for the Sudbury area (Pearson 1985). The term F is the weight fraction of magmatic fluid added to parental groundwater. For example, a mixture that contains 10% magmatic fluid by mass has $F = 0.1$. The remainder of the fluid mixture ($1 - F = 0.9$) is parental groundwater.

Where the three mixing curves overlie the leachate data (Fig. 14), both compositional trends 1 and 2 may be explained. Mixing of groundwater with only one of the magmatic fluid components with a fixed Cl:Br does not explain the data. This scenario could result from the mixing of groundwater with several pulses of magmatic fluid, or with a magmatic fluid whose Cl:Br ratio continuously decreased after exsolution (*i.e.*, by the removal of Cl from the fluid during growth of silicate minerals). According to the model, up to 80 wt% of the mixture must be a magmatic fluid component in order to lower the Ca:Na ratio in the hybrid fluid sufficiently to account for all of the leachate compositions.

If multiple pulses of hydrothermal activity during the waning stages of magmatism succeeded in transporting fluids with elevated Cl:Br ratios into the footwall (from leaching of the SIC rocks) or if such a high-(Cl:Br) ratio fluid was exsolved directly from the SIC during its crystallization, then mixing of this fluid with groundwater may explain the range in Cl:Br ratios observed in the leachates that follow trends 1 and 2. Entrapment of this hybrid fluid during the recrystallization of the Sudbury Breccia by contact metamorphism or migration of hydrothermal fluid in ore-bearing breccia zones occurred along grain boundaries in the matrix of the breccias (forming type-II inclusions). The presence of elevated abundances of the trapped hybrid fluid near ore is supported by other indications that zones of Sudbury Breccia that presently host footwall ores also served as conduits for the migration of hydrothermal fluid (Morrison *et al.* 1994, Hanley 2002, Hanley & Mungall 2003). Evidence for this in samples of Sudbury Breccia near ore are the large volumes of Cl-bearing silicate minerals in the Sudbury Breccia matrix (Hanley & Mungall 2003), increased abundances of grain-margin-hosted fluid inclusions, and increased concentrations of soluble constituents with increasing proximity to ore. The entrapment of the hybrid fluid in the matrix of the Sudbury Breccia during its recrystallization was not a process restricted to Sudbury Breccia near ore, since leachates from distal samples also demonstrate high Cl:Br and low Ca:Na ratios.

It remains unclear why a fluid originating from SIC magma would have had an elevated Cl:Br ratio compared to trapped fluids occurring in the target rocks that generated the SIC magma (the same fluids that were leached to generate the composition of deep groundwaters in the area). One possibility is that the SIC melt sheet inherited its Cl:Br ratio from seawater, which is known to have covered the target area (Ames 1999) and might be expected to have a high Cl:Br ratio (modern seawater has a Cl:Br ratio of approximately 280: Lahermo & Lampen 1987).

An alternative source for magmatic fluids with high Cl:Br ratios could be the footwall sulfide ores themselves. In a recent experimental study, Mungall & Brenan (2003) demonstrated that Cl and Br partition into sulfide liquid and the Nernst partition coefficient for Cl between sulfide and silicate melt is approximately twice that of Br. Therefore, aqueous fluid phase exsolved from crystallizing sulfide may have inherited a high Cl:Br ratio from a high Cl:Br parent sulfide liquid. The high Cl content of the sulfide liquid that formed the footwall-style Cu–Ni–PGE ores in the study area is supported in part by the observation of inclusions (phenocrysts?) of Fe-chloride and Cl-rich pyrosmalite [ideal formula: $(\mathrm{Fe}^{2+},\mathrm{Mn})_8\mathrm{Si}_6\mathrm{O}_{15}(\mathrm{OH},\mathrm{Cl})_{10}$] in massive sulfide in the footwall ore-zones (Li 1992, Farrow 1994, Farrow & Watkinson 1999).

CONCLUSIONS

In this study, we have shown that there is a distinct enrichment in bulk-rock and water-soluble (at 20°C) Cl and Br, and an increase in bulk Cl:Br ratio in the matrix of Sudbury Breccia *in heavily brecciated units* within 150 m of footwall style Cu–Ni–PGE ores at the Fraser mine. Concentrations of bulk Cl and Br should be considered anomalous if they exceed the threshold values of 357 ppm and 3.2 ppm, respectively. Cl:Br ratios in the bulk rock are controlled primarily by the insoluble minerals in the matrix, which have been shown to increase in abundance near ore (Hanley & Mungall 2003), and which preferentially concentrated Cl relative to Br during their growth. This preferential concentration of Cl and corresponding increase in the Cl:Br ratio of the Sudbury Breccia matrix does not require any equilibrating fluids to have had anomalously high Cl:Br ratios.

A significant portion of the bulk Cl and Br present in the breccia matrix is water-soluble at room temperature. Although concentrations of soluble Cl and Br in the matrix increase with proximity to ore, there is no correlation between Cl:Br ratios in aqueous leachates and proximity to ore. However, Cl:Br ratios in the leachates have a wide range of values (83.2 to 308.6) compared to the range observed in Sudbury groundwaters. The range in leachate compositions may be explained by the presence of trapped mixtures of groundwater (the Ca^{2+}-dominant end-member) and up to 80 wt% of another fluid (the Na^+ and K^+-dominant end-member, possibly SIC-derived), which had an elevated and variable Cl:Br ratio. Entrapment of the hybrid fluid component may have occurred during the recrystallization of the Sudbury Breccia during contact metamorphism and migration of the hybrid fluid. This process was common to the entire footwall, but in ore-bearing breccia zones, fluid migration was clearly enhanced (*i.e.*, greater density of microfractures), as indicated by the elevated abundances of grain-boundary-hosted vapor-rich fluid inclusions occurring in patches of quartz in the matrix of the breccias near ore, and the increase in the concentration of soluble constituents with proximity to ore. As an alternative to a hybrid fluid model, the entrapment (by matrix recrystallization) of small amounts ($<10^{-5}$ wt%) of halite deposited by halite-saturated groundwater may artificially increase the Cl:Br ratio in the soluble halogen fraction of the breccia matrix, mimicking the presence of a trapped high Cl:Br fluid.

ACKNOWLEDGEMENTS

The authors thank Paul Binney and John Fedorowich of Falconbridge Ltd. (both at the Sudbury Exploration Office) for their guidance and logistical support, and Dave King, Kevin Chisholm, and Al Wilkins of Falconbridge Ltd. (geology department of the Fraser and Strathcona mines) for their permission and assistance in accessing underground workings for sampling purposes. Funding for J.M. from Falconbridge Ltd. and NSERC is gratefully acknowledged. Support for J.H. came in the form of an Ontario Graduate Scholarship in Science and Technology and the H. Ellsworth Scholarship in Mineralogy (Department of Geology, University of Toronto). The manuscript was greatly improved through reviews by A. Boudreau, C.E.G. Farrow, P.G. Spry, and R.F. Martin.

REFERENCES

AMES, D.E. (1999): *Geology and Regional Hydrothermal Alteration of the Crater-Fill, Onaping Formation: Association with Zn–Pb–Cu Mineralization, Sudbury Structure, Canada*. Ph.D. thesis, Carleton Univ., Ottawa, Ontario.

BASHARINA, L.A. (1965): Gases of Kamchatka volcanoes. *Bull. Volcanol.* **28**, 95-105.

BOHLKE, J.K. & IRWIN, J.J. (1992): Laser microprobe analyses of Cl, Br, I, and K in fluid inclusions: implications for sources of salinity in some ancient hydrothermal fluids. *Geochim. Cosmochim. Acta* **56**, 203-225.

BOTTRELL, S.H. & YARDLEY, B.W.D. (1988): The composition of a primary granite-derived ore fluid from S.W. England, determined by fluid inclusions analysis. *Geochim. Cosmochim. Acta* **52**, 585-588.

BUCHAN, R. (1981): Mineralogical examination of samples from Strathcona mine footwall copper zone. *Falconbridge Nickel Mines Internal Report, Project* **301**.

CHANNER, D.M.D., BRAY, C.J. & SPOONER, E.T.C. (1994): Integrated cation–anion/volatile fluid inclusion analysis by gas and ion chromatography; methodology and examples. *Chem. Geol.* **154**, 59-82.

COATS, C.J.A. & SNAJDR, P. (1984): Ore deposits of the North Range, Onaping – Levack area. *In* The Geology and Ore Deposits of the Sudbury Structure (E.G. Pye, A.J. Naldrett & P.E. Giblin, eds.). *Ontario.Geol. Surv., Spec. Vol.* **1**, 327-346.

CORRENS, C.W. (1956): The geochemistry of the halogens. *Phys. Chem. Earth* **1**, 181-233.

COWAN, J.C. (1968): Geology of the Strathcona ore deposit. *Can. Inst. Mining Metall. Bull.* **61**(669), 38-54.

DIETZ, R.S. (1964): Sudbury structure an astrobleme. *J. Geol.* **72**, 412-434.

DRESSLER, B.O. (1984): The effects of the Sudbury event and the intrusion of the Sudbury Igneous Complex on the footwall rocks of the Sudbury Structure. *In* The Geology and Ore Deposits of the Sudbury Structure (E.G. Pye, A.J. Naldrett & P.E. Giblin, eds.). *Ontario Geol. Surv., Spec. Vol.* **1**, 97-136.

FARROW, C.E.G. (1994): *Geology, Alteration, and the Role of Fluids in Cu–Ni–PGE Mineralization of the Footwall Rocks to the Sudbury Igneous Complex, Levack and Morgan Townships, Sudbury District, Ontario*. Ph.D. thesis, Carleton Univ., Ottawa, Ontario.

________ & WATKINSON, D.H. (1992): Alteration and the role of fluids in Ni, Cu, and platinum-group element deposition, Sudbury Igneous Complex contact, Onaping–Levack area, Ontario. *Mineral. Petrol.* **46**, 67-83.

________ & ________ (1996): Geochemical evolution of the epidote zone, Fraser mine, Sudbury, Ontario: Ni–Cu–PGE remobilization by saline fluids. *Explor. Mining Geol.* **5**, 17-31.

________ & ________ (1997): Diversity of precious-metal mineralization in footwall Cu–Ni–PGE deposits, Sudbury, Ontario; implications for hydrothermal models of formation. *Can. Mineral.* **35**, 817-839.

________ & ________ (1999): An evaluation of the role of fluids in Ni–Cu–PGE-bearing, mafic-ultramafic systems. *In* Dynamic Processes in Magmatic Ore Deposits and their Application to Mineral Exploration (R.R. Keays, C.M. Lesher, P.C. Lightfoot & C.E.G. Farrow, eds.). *Geol. Assoc. Can., Short Course Notes* **13**, 31-67.

FEDOROWICH, J.S., ROUSELL, D.H. & PEREDERY, W.V. (1999): Sudbury Breccia distribution and orientation in an embayment environment. *Geol. Soc. Am., Spec. Pap.* **339**, 305-315.

FRAPE, S.K. & FRITZ, P. (1982): The chemistry and isotopic composition of saline groundwaters from the Sudbury basin, Ontario. *Can. J. Earth Sci.* **19**, 645-661.

________ & ________ (1987): Geochemical trends from groundwaters from the Canadian Shield. *In* Saline Water and Gases in Crystalline Rocks (P. Fritz & S.K. Frape, eds.). *Geol. Assoc. Can.*, *Spec. Pap.* **33**, 19-38.

GASCOYNE, M., DAVISON, C.C., ROSS, J.D. & PEARSON, R. (1987): Saline groundwaters and brines in plutons in the Canadian Shield. *In* Saline Water and Gases in Crystalline Rocks (P. Fritz & S.K. Frape, eds.). *Geol. Assoc. Can.*, *Spec. Pap.* **33**, 53-68.

GRIEVE, R.A.F. (1994): An impact model of the Sudbury Structure. *In* Proceedings of the Sudbury – Noril'sk Symposium (P.C. Lightfoot & A.J. Naldrett, eds.). *Ontario Geol. Surv., Spec. Vol.* **5**, 119-132.

GUHA, J. & KANWAR, R. (1987): Vug brines – fluid inclusions: a key to the understanding of secondary gold enrichment processes and the evolution of deep brines in the Canadian Shield. *In* Saline Water and Gases in Crystalline Rocks (P. Fritz & S.K. Frape, eds.). *Geol. Assoc. Can.*, *Spec. Pap.* **33**, 95-119.

HANLEY, J.J. (2002): *The Distribution of the Halogens in Sudbury Breccia Matrix as a Pathfinder Elements for Footwall Cu–PGE Mineralization at the Fraser Cu Zone, Barnet Main Copper Zone, and Surrounding Margin of the Sudbury Igneous Complex, Onaping–Levack Area, Ontario, Canada.* M.Sc. thesis, Univ. of Toronto, Toronto, Ontario.

________ & MUNGALL, J.E. (2003): Chlorine enrichment and hydrous alteration of the Sudbury Breccia hosting footwall Cu–Ni–PGE mineralization at the Fraser mine, Sudbury, Ontario, Canada. *Can. Mineral.* **41**, 857-881.

JAGO, B.C., MORRISON, G.G. & LITTLE, T.L. (1994): Metal zonation patterns and microtextural and micromineralogical evidence for alkali- and halogen-rich fluids in the genesis of the Victor Deep and McCreedy East footwall copper ore bodies, Sudbury Igneous Complex. *In* Proceedings of the Sudbury – Noril'sk Symposium (P.C. Lightfoot & A.J. Naldrett, eds.). *Ontario Geol. Surv., Spec. Vol.* **5**, 65-75.

KRAFT, K. & CHAIGNEAU, M. (1976): Chlorine–bromine ratios of volcanic gas from twelve Indonesian volcanoes (Sumatra, Java, Flores, and Sulawesi). *C.R. Acad. Sci. Paris* **282**, *Sér.* **D**, 341-343.

KROGH, T.E., DAVIS, D.W. & CORFU, F. (1984): Precise U–Pb zircon and baddeleyite ages for the Sudbury area. *In* The Geology and Ore Deposits of the Sudbury Structure (E.G. Pye, A.J. Naldrett & P.E. Giblin, eds.). *Ontario Geol. Surv., Spec. Vol.* **1**, 431-446.

LAHERMO, P.W. & LAMPEN, P.H. (1987): Brackish and saline groundwaters in Finland. *In* Saline Water and Gases in Crystalline Rocks (P. Fritz & S.K. Frape, eds.). *Geol. Assoc. Can., Spec. Pap.* **33**, 103-110.

LI, CHUSI (1992): *A Quantitative Model for the Formation of Sulfide Ores at Sudbury and a Study on the Distributions of Platinum-group Elements in the Strathcona Copper-Rich Zones, Sudbury, Ontario*. Ph.D. thesis, Univ. of Toronto, Toronto, Ontario.

________ & NALDRETT, A.J. (1993): High chlorine alteration minerals and calcium-rich brines in fluid inclusions from the Strathcona deep copper zone, Sudbury, Ontario. *Econ. Geol.* **88**, 1780-1796.

MARSHALL, D., WATKINSON, D., FARROW, C., MOLNÁR, F. & FOUILLAC, A.-M. (1999): Multiple fluid generations in the Sudbury Igneous Complex: fluid inclusion, Ar, O, H, Rb and Sr evidence. *Chem. Geol.* **154**, 1-19.

MCCORMICK, K.A., LESHER, C.M., MCDONALD, A.M., FEDOROWICH, J.S. & JAMES, R.S. (2002): Chlorine and alkali geochemical halos in the footwall breccia and sublayer norite at the margin of the Strathcona embayment, Sudbury Structure, Ontario. *Econ. Geol.* **97**, 1509-1519.

________ & MCDONALD, A.M. (1999): Chlorine-bearing amphiboles from the Fraser mine, Sudbury, Ontario, Canada: description and crystal chemistry. *Can. Mineral.* **37**, 1385-1403.

MOLNÁR, F., WATKINSON, D.H. & JONES, P.C. (2001): Mutiple hydrothermal processes in footwall units of the North Range, Sudbury Igneous Complex, Canada, and implications for the genesis of vein-type Cu–Ni–PGE deposits. *Econ. Geol.* **96**, 1645-1670.

MORRISON, G.G., JAGO, B.C. & WHITE, T.L. (1994): Footwall mineralization of the Sudbury Igneous Complex. *In* Proceedings of the Sudbury – Noril'sk Symposium (P.C. Lightfoot & A.J. Naldrett, eds.). *Ontario Geol. Surv., Spec. Vol.* **5**, 57-64.

MUNGALL, J.E. & BRENAN, J.M. (2003): Experimental evidence for the chalcophile behavior of the halogens. *Can. Mineral.* **41**, 207-220.

PEARSON, F.J., JR. (1985): Geochemical and isotopic evidence on the origin of brines in the Canadian Shield. Report by INTERA Technologies, Inc., Texas for Atomic Energy of Canada, Ltd., Pinawa, Manitoba.

ROEDDER, E. (1984): Fluid Inclusions. *Rev. Mineral.* **12**.

SHAND, S.J. (1916): The pseudotachylite of Parijs (Orange Free State). *Geol. Soc. London, Quart. J.* **72**, 198-221.

SIEMANN, M.G. & SCHRAMM, M. (2000): Thermodynamic modeling of the Br partition between aqueous solutions and halite. *Geochim. Cosmochim. Acta* **64**, 1681-1693.

SNYDER, G.T. & FEHN, U. (2002): Origin of iodine in volcanic fluids: ^{129}I results from the Central American Volcanic Arc. *Geochim. Cosmochim. Acta* **66**, 3827-3838.

SPRAY, J.G. (1997): Superfaults. *Geology* **25**, 579-582.

SPRINGER, G. (1989): Chlorine-bearing and other uncommon minerals in the Strathcona Deep Copper Zone, Sudbury District, Ontario. *Can. Mineral.* **27**, 311-313.

STONE, M. & EXLEY, C.S. (1985): High heat production granites of southwest England and their associated mineralization: a review. *In* High Heat Production (HHP) Granites, Hydrothermal Circulation, and Ore Genesis. *Inst. Mining Metall., Spec. Publ.*, 571- 593.

SUGIURA, T., MIZUTANI, Y. & OANA, S. (1963): Fluorine, chlorine, bromine, and iodine in volcanic gases. *J. Earth Sci. Nagoya Univ.* **11**, 272 (abstr.).

WILSHIRE, H.G. (1971): Pseudotachylites from the Vredefort ring, South Africa, and the origins of lunar breccia. *Geol. Soc. Am., Bull.* **94**, 926-935.

YOSHIDA, M., TAKAHASHI, K., YONEHARA, N. & IWASAKI, I. (1965): The fractionation of halogen compounds through the process of volatilization and the sublimation from volcanic rocks on heating. *Bull. Chem. Soc. Japan* **38**, 1436 (abstr.).

________, ________, ________, OZAWA, T. & IWASAKI, I. (1971): The fluorine, chlorine, bromine, and iodine contents of volcanic rocks. *Bull. Chem. Soc. Japan* **44**, 1844-1850.

Received March 20, 2004, revised manuscript accepted September 15, 2004.